

1 **Mg/Ca, Sr/Ca AND STABLE ISOTOPES FROM THE PLANKTONIC**
2 **FORAMINIFERA *T. SACCULIFER*: TESTING A MULTI-PROXY APPROACH FOR**
3 **INFERRING PALEO-TEMPERATURE AND PALEO-SALINITY**
4
5

6 Delphine Dissard (1, 2), Gert Jan Reichart (3, 4), Christophe Menkes (5), Morgan Mangeas (5), Stephan
7 Frickenhaus (2) and Jelle Bijma (2)

8
9 (1) UMR LOCEAN (IRD-CNRS-MNHN-Sorbonne Université), Centre IRD de Nouméa 101 Promenade Roger Laroque,
10 Noumea 98848, New Caledonia.

11 (2) Alfred-Wegener-Institute, Helmholtz-Zentrum für Polar- und Meeres Forschung, Am Handelshafen 12, 27570
12 Bremerhaven, Germany

13 (3) NIOZ Royal Netherlands Inst. Sea Res, Den Burg, Texel, Netherlands.

14 (4) Univ. Utrecht, Fac Geosci. Dept Earth Sci. Utrecht, Netherlands

15 (5) UMR ENTROPIE (IRD, Univ. de la Réunion, CNRS, IFREMER, UNC), Centre IRD de Nouméa 101 Promenade Roger
16 Laroque, Noumea 98848, New Caledonia.
17

18
19
20
21
22 **ABSTRACT**
23

24 Over the last decades, sea surface temperature (SST) reconstructions based on the Mg/Ca of
25 foraminiferal calcite have frequently been used in combination with the $\delta^{18}\text{O}$ signal from the
26 same material, to provide estimates of $\delta^{18}\text{O}$ of the water ($\delta^{18}\text{O}_w$), a proxy for global ice volume
27 and sea surface salinity (SSS). However, because of error propagation from one step to the next,
28 better calibrations are required to increase accuracy and robustness of existing isotope and
29 element to temperature proxy-relationships. Towards that goal, we determined Mg/Ca, Sr/Ca
30 and the oxygen isotopic composition of *Trilobatus sacculifer* (previously referenced as
31 *Globigerinoides sacculifer*), collected from surface waters (0-10m), along a North-South
32 transect in the eastern basin of the tropical/subtropical Atlantic Ocean. We established a new
33 paleo-temperature calibration based on Mg/Ca, and on the combination of Mg/Ca and Sr/Ca.
34 Subsequently, a sensitivity analysis was performed in which, one, two, or three different
35 equations were considered. Results indicate that foraminiferal Mg/Ca allow for an accurate
36 reconstruction of surface water temperature. Combining equations, $\delta^{18}\text{O}_w$ can be reconstructed
37 with a precision of about $\pm 0.5\%$. However, the best possible salinity reconstruction based on
38 locally calibrated equations, only allowed reconstruction with an uncertainty of ± 2.49 . This was
39 confirmed by a Monte Carlo simulation, applied to test successive reconstructions in an ‘ideal
40 case’, where explanatory variables are known. This simulation shows that from a pure statistical
41 point of view, successive reconstructions involving Mg/Ca and $\delta^{18}\text{O}_c$ preclude salinity

42 reconstruction with a precision better than ± 1.69 and hardly better than ± 2.65 , due to error
43 propagation. Nevertheless, a direct linear fit to reconstruct salinity based on the same measured
44 variables (Mg/Ca and $\delta^{18}O_c$) was established. This direct reconstruction of salinity lead to a
45 much better estimation of salinity (± 0.26) than the successive reconstructions.

46

47

48

I. INTRODUCTION

49

50 Since Emiliani's pioneering work (1954), oxygen isotope compositions recorded in fossil
51 foraminiferal shells became a major tool to reconstruct past sea surface temperature. After
52 Shackleton's seminal studies (1967, 1968 and 1974), it became clear that part of the signal
53 reflected glacial-interglacial changes in continental ice volume and hence sea level variations.
54 The oxygen isotope composition of foraminiferal calcite ($\delta^{18}O_c$) is thus controlled by the
55 temperature of calcification (Urey, 1947; Epstein et al., 1953) but also by the oxygen isotope
56 composition of seawater ($\delta^{18}O_w$). The relative contribution of these two factors cannot be
57 deconvolved without an independent measure of the temperature at the time of calcification
58 such as e.g. Mg/Ca (e.g. Nürnberg et al., 1996; Rosenthal et al., 1997; Rathburn and DeDeckker,
59 1997; Hastings et al., 1998; Lea et al., 1999; Lear et al., 2002; Toyofuku et al., 2000; Anand et
60 al., 2003, al., Kisakurek et al., 2008; Duenas-Bohorquez et al., 2009, 2011; Honisch et al., 2013;
61 Kontakiotis et al., 2016; Jentzen et al., 2018). The sea surface temperature (SST) reconstructed
62 from Mg/Ca of foraminiferal calcite has, therefore, increasingly been used in combination with
63 the $\delta^{18}O$ signal measured on the same material, to estimate $\delta^{18}O_w$, global ice volume and to
64 infer past sea surface salinity (SSS) (e.g. Rohling 2000, Elderfield and Ganssen, 2000; Schmidt
65 et al., 2004; Weldeab et al., 2005; 2007). These studies also showed that, because of error
66 propagation, inaccuracies in the different proxies combined for the reconstruction of past sea
67 water $\delta^{18}O$ and salinity obstruct meaningful interpretations. Hence, while there is an
68 understandable desire to apply empirical proxy-relationships down-core, additional calibrations
69 appear necessary to make reconstructions more robust. Calibrations using foraminifera sampled
70 from surface seawater (0-10m deep), provide the best possibility to avoid most of the artefacts
71 usually seen when using specimen from core tops or culture experiments for calibration
72 purposes. Here, we report a calibration based on *Globigerinoides sacculifer*, which should now
73 and will be referenced in this manuscript as *Trilobatus sacculifer* (Spezzaferrri et al., 2015),
74 from the Atlantic Ocean. Mg and Sr concentrations were measured on the last chamber of
75 individual specimens with Laser Ablation-Inductively Coupled Plasma-Mass Spectrometry

76 (LA-ICP-MS), while the oxygen isotope composition of the same tests as used for the elemental
77 analyses was subsequently measured by Isotope ratio Mass Spectrometry (IRMS).
78 Environmental parameters (temperature: T, salinity: S, dissolved inorganic carbon: DIC and
79 alkalinity: ALK) but also the isotopic composition (O^{18}_w) of the seawater the foraminifera were
80 growing in, were measured. The primary objectives of this study are (1) to test and improve the
81 calibration of both the Mg/Ca and oxygen isotope paleothermometer for the paleoceanographic
82 relevant species *T. sacculifer*; (2) to test whether the incorporation of Sr into the Mg-T
83 reconstruction equation improves temperature reconstruction by accounting for the impact of
84 salinity; (3) evaluate the agreement between observed and predicted $\delta^{18}O_w$ and (4) test potential
85 for SSS reconstructions of the Atlantic Ocean. Our results indicate that the best possible salinity
86 reconstruction based on locally calibrated equations from the present study, only allowed
87 reconstruction with an uncertainty of ± 2.49 . Such an uncertainty does not allow for viable
88 (paleo)salinity data. This is subsequently confirmed by a Monte Carlo simulation, applied to
89 test successive reconstructions in an ‘ideal case’, where explanatory variables are known. This
90 simulation shows that from a pure statistical point of view, successive reconstructions involving
91 Mg/Ca and $\delta^{18}O_c$ preclude salinity reconstruction with a precision better than ± 1.69 and hardly
92 better than ± 2.65 , due to error propagation. Nevertheless, a direct linear fit based on the same
93 measured variables (Mg/Ca and $\delta^{18}O_c$), and leading to much better estimation of salinity
94 (± 0.26), could be established.

95

96

2. MATERIAL AND METHODS

97

2.1. Collection procedure

99 Foraminifera were collected between October and November 2005, on board of the research
100 vessel Polarstern (ANT XXIII/1) during a meridional transect of the Atlantic Ocean
101 (Bremerhaven/Germany - Cape Town/South of Africa; Fig. 1a). Foraminifera were
102 continuously collected from a depth of ca. 10 m using the ship’s membrane pump (3 m³/h). The
103 water flowed into a plankton net (125 μ m) that was fixed in a 1000 L plastic tank with an
104 overflow (Fig 1b). Every eight hours, the plankton accumulated in the net was collected.
105 Temperature and salinity of surface seawaters were continuously recorded by the ship’s
106 systems, and discrete water samples were collected for later analyses of total ALK, DIC and
107 $\delta^{18}O_w$ (see Tab. 1). Plankton and water samples were poisoned with buffered formaldehyde
108 solution (20%) and HgCl₂ (1.5 ml with 70gL⁻¹ HgCl₂ for 1 L samples), respectively. In total,
109 more than seventy plankton samples were collected during the transect, covering a large range

110 in both temperature and salinity. Specimens of *T. sacculifer* from thirteen selected stations,
111 selected as to maximize temperature and salinity ranges, were picked and prepared for analyses.
112 Salinity, temperature, DIC, ALK and $\delta^{18}\text{O}_w$ data reported in this paper represent
113 October/November values for the selected stations.

114

115 **2.2. Description of species**

116 *Trilobatus sacculifer* is a spinose species with endosymbiotic dinoflagellates inhabiting the
117 shallow (0-80 m deep) tropical and subtropical regions of the world oceans. This species
118 displays a large tolerance to temperature (14-32°C) and salinity (24-47) (Hemleben et al., 1989;
119 Bijma et al., 1990). Based on differences in the shape of the last chamber of adult specimens,
120 various morphotypes can be distinguished. Among others the last chamber can be smaller than
121 the penultimate chamber, in which case it is called kummerform (kf). This species shows an
122 ontogenetic depth migration and predominantly reproduces at depth around full moon (Bijma
123 and Hemleben, 1993). Just prior to reproduction a secondary calcite layer, called gametogenic
124 (GAM) calcite is added (Bé et al., 1982; Bijma and Hemleben, 1993; Bijma et al., 1994).
125 Juveniles (<100 μm) ascend in the water column and reach the surface after less than
126 approximately 2 weeks. Pre-adult stages then slowly descend within 9-10 days to the
127 reproductive depth. In our samples (collected between 0 and 10 m depth), *T. sacculifer*
128 specimens have not yet added the Mg-enriched gametogenic calcite, which generally occurs
129 deeper in the water column just prior to reproduction. Therefore, only the trilobus morphotype
130 without GAM calcite is considered in this study, which limits the environmental, ontogenetic
131 and physiological variability between samples even if a rather wide size fraction (230 to
132 500 μm) was selected due to sample size limitation. This should be taken into account when
133 compared to other calibrations based on core top and/or sediment trap collected specimen

134

135 **2.3. Seawater analysis**

136 The DIC and ALK analyses of the sea water were carried out at the Leibniz Institute of Marine
137 Sciences at the Christian-Albrechts University of Kiel, (IFM-GEOMAR), Germany. Analyses
138 were performed by extraction and subsequent coulometric titration of evolved CO_2 for DIC
139 (Johnson et al., 1993), and by open-cell potentiometric seawater titration for ALK (Mintrop et
140 al., 2000). Precision / accuracy of DIC and ALK measurements are 1 $\mu\text{mol kg}^{-1}$ / 2 $\mu\text{mol kg}^{-1}$
141 and 1.5 $\mu\text{mol kg}^{-1}$ / 3 $\mu\text{mol kg}^{-1}$, respectively. Accuracy of both DIC and ALK was assured by
142 the analyses of certified reference material (CRM) provided by Andrew Dickson from Scripps
143 Institution of Oceanography, La Jolla, USA. Measurements of $\delta^{18}\text{O}_w$ were carried out at the

144 Faculty of Geosciences, Utrecht University, Netherlands. Samples were measured using a
145 GasBench II - Delta plus XP combination. Results were corrected for drift with an in-house
146 standard (RMW) and are reported on V-SMOW scale, with a precision of 0.1‰ and accuracy
147 verified against NBS 19 of 0.2‰ respectively. For reconstruction calculations $\delta^{18}\text{O}$ data were
148 corrected to the PDB scale by subtracting 0.27‰ (Hut, 1987).

149

150 **2.4. Carbonate analysis**

151 2.4.1. Foraminiferal sample preparation

152 Under a binocular microscope, maximum test diameter of each specimen was measured and
153 individual tests were weighed on a microbalance (METTLER TOLEDO, precision $\pm 0.1\mu\text{g}$).
154 Since the foraminifera were never in contact with sediments, the rigorous cleaning procedure
155 required for specimens collected from sediment cores, was not necessary. Prior to analysis the
156 tests were cleaned following a simplified cleaning procedure: All specimens were soaked for
157 30 min in a 3-7% NaOCl solution (Gaffey and Brönniman, 1993). A stereomicroscope was used
158 during cleaning and specimens were removed from the reagent directly after complete
159 bleaching. The samples were immediately and thoroughly rinsed with deionised water to ensure
160 complete removal of the reagent. After cleaning, specimens were inspected with scanning
161 electron microscopy and showed no visible signs of dissolution. This cleaning procedure
162 preserves original shell thickness and thus maximises data acquisition during laser ablation.
163 Foraminifera were fixed on a double-sided adhesive tape and mounted on plastic stubs for LA-
164 ICP-MS analyses.

165

166 2.4.2. Elemental composition analysis

167 For each station, 5–13 specimens were analysed. Their last chambers were ablated using an
168 Excimer 193 nm deep ultraviolet laser (Lambda Physik) with GeoLas 200Q optics (Reichert et
169 al, 2003) creating 80 μm diameter craters. Pulse repetition rate was set at 6 Hz, with an energy
170 density at the sample surface of 1 J/cm^2 . The ablated material was transported on a continuous
171 helium flow into the argon plasma of a quadrupole ICP-MS instrument (Micromass Platform)
172 and analysed with respect to time. Ablation of calcite requires ultraviolet wavelengths as an
173 uncontrolled disruption would result from higher wavelengths. By using a collision and reaction
174 cell spectral interferences on the minor isotopes of Ca (^{42}Ca , ^{43}Ca and ^{44}Ca) were reduced and
175 interferences of clusters like $^{12}\text{C}^{16}\text{O}^{16}\text{O}$ were prevented. Analyses were calibrated against NIST
176 (U.S. National Institute of Standards and Technology) 610 glass using the concentration data
177 of Jochum et al. (2011) with Ca as internal standard. For Ca quantification, mass 44 was used

178 while monitoring masses 42 and 43 as internal check. In the calcite, the Ca concentration was
179 set at 40%, allowing direct comparison to trace metal/Ca from traditional wet-chemical studies.
180 Mg concentrations were calculated using masses 24 and 26; Sr concentrations were calculated
181 with mass 88. One big advantage in using LA-ICP-MS measurements is that single laser pulses
182 remove only a few nanometers of material, which allows high resolution trace elements profiles
183 to be acquired (e.g. Reichart et al., 2003; Regenberg et al., 2006; Dueñas-Bohórquez et al.,
184 2009, 2010, Hathorne et al., 2009; Munsel et al., 2010; Dissard et al., 2009; 2010a and b; Evans
185 et al., 2013; 2015; Steinhardt 2014, 2015; Fehrenbacher et al., 2015; Langer et al., 2016; Koho
186 et al., 2015; 2017; Fontanier et al., 2017; De Nooijer et al., 2007, 2014, 2017a and b; Jentzen et
187 al., 2018, Schmitt et al., 2019; Levi et al., 2019). Element concentrations were calculated for
188 the individual ablation profiles integrating the different isotopes (glitter software). Even though
189 the use of a single or very few specimens, can be criticised when determining foraminifera
190 Mg/Ca and $\delta^{18}\text{O}$ in order to perform paleoclimate reconstructions instead of more traditional
191 measurements, Groeneveld et al., (2019) recently demonstrated that for both proxies, single
192 specimen variability is dominated by seawater temperatures during calcification, even if the
193 presence of an ecological effect leading to site-specific seasonal and depth habitat changes is
194 also noticeable.

195

196 **2.5. Stable isotope analysis**

197 The specimens used for elemental composition analyses using LA-ICP-MS were subsequently
198 carefully removed from the plastic stubs and rinsed with deionised water before measuring their
199 stable isotope composition. Depending on shell weight, 2 to 3 foraminifera were necessary to
200 obtain a minimum of 20 μg of material, required for each analysis. Analyses were carried out in
201 duplicate for each station. The results, compiled in table 2, represent average measurements.
202 The analyses were carried out at the Department of Earth Sciences of Utrecht University (The
203 Netherlands), using a Kiel-III -Finnigan MAT-253 mass spectrometer combination. The $\delta^{18}\text{O}_\text{c}$
204 results are reported in ‰ PDB. Calibration was made with NBS-19 (precision of 0.06-0.08 ‰
205 for sample size 20-100 μg , accuracy better than 0.2‰).

206

207 **2.6. Statistical analysis**

208 Within this manuscript, all statistical analyses with regards to elemental and isotopic data, were
209 carried out using the program R with default values (R Development Core Team (2019)).

210

211

3. RESULTS

212

213 3.1. Elemental composition

214 Overall values of the Mg/Ca and Sr/Ca ratios in the tests of *T. sacculifer* varied from 1.78 to
215 5.86 mmol/mol (Fig. 2a) and 1.41 to 1.52 mmol/mol (fig. 2b), respectively (Tab. 2). These
216 Mg/Ca concentrations compare well with results found in literature for this species from either
217 culture experiments, plankton tow, or surface sediment, growing at the same temperatures (e.g.
218 Nürnberg et al., 1996; Anand et al. 2003, Regenberg et al., 2009, Fig. 3). Similarly, the overall
219 variation in Sr/Ca-values reported in this study is comparable to that observed in core top and
220 cultured *G. ruber* and *T. sacculifer* combined, for comparable salinity and temperature
221 conditions, (varying between 1.27 to 1.51mmol/mol; e.g. Cleroux et al., 2008; Kısakürek et al.,
222 2008; Dueñas-Bohórquez et al., 2009).

223

224 The relationship between both Mg/Ca and Sr/Ca ratios and measured temperatures were
225 calculated using least square differences. Both show a good correlation with surface water
226 temperature (Fig. 2, Tab. 3). The Mg/Ca ratio increases exponentially by 8.3%/°C (best fit)
227 (Mg/Ca and Sr/Ca ratios given in mmol/mol):

$$228 \text{Mg/Ca}=(0.42\pm 0.13) \exp((0.083\pm 0.001)*T), R^2=0.86 \quad \text{pvalue}=2,9\text{e-}06 \quad (\text{equation 1})$$

229

230 whereas Sr/Ca ratio increases linearly by 0.6%/°C (Fig. 2a and b), best fit:

$$231 \text{Sr/Ca}=(0.009\pm 0.002)*T+(1.24\pm 0.05), R^2=0.67 \quad \text{pvalue}=5.\text{e-}04 \quad (\text{equation 2})$$

233

234 Concerning the temperature reconstruction, by inverting the approach, univariate regressions
235 yields to:

$$236 T=(12.3\pm 1.5)+((10.5\pm 1.2)*\log(\text{Mg/Ca}), R^2=0.86 \quad \text{pvalue}=2,9\text{e-}06 \quad (\text{equation 1'})$$

237 And

$$238 T=+(-84.1\pm 22.9)+((71.7\pm 15)*\text{Sr/Ca}), R^2=0.67 \quad \text{pvalue}=5\text{e-}04 \quad (\text{equation 2'})$$

239

240 Combining Mg and Sr data for a non-linear multivariate regression allows improvement of the
241 correlation with temperature, best fit:

242

$$243 T=- (27\pm 15)+ (8\pm 1)*\ln(\text{Mg/Ca})+(28\pm 11)*\text{Sr/Ca}, \text{pvalue Mg/Ca: } 2.10^{-4} \quad (\text{equation 3})$$

244

$$R^2=0.93 \quad \text{pvalue}= 2.\text{e-}04$$

245 For comparison, with regression found in the literature, Mg/Ca is estimated below as a function
246 of temperature and Sr/Ca:

$$247 \quad \text{Mg/Ca} = \exp((0.98 \pm 1.89) + (0.09 \pm 0.02) * T + (-1.43 \pm 1.45) * \text{Sr/Ca})$$
$$248 \quad R^2 = 0.86 \quad \text{pvalue} = 2.05e-05 \quad (\text{equation 3'})$$

249
250 Regression for the relationship between salinity and Mg/Ca ratios does not show any clear
251 correlation ($R^2=0.09$, $p\text{-value}=0.32$). This is in good agreement with previous culture
252 experiments studies which only report a minor sensitivity of Mg/Ca to salinity in planktonic
253 foraminifera (e.g. Dueñas-Bohórquez et al., 2009; Hönisch et al., 2013; Kisakürek et al., 2008;
254 Nürnberg et al., 1996). The correlation observed between Sr/Ca ratios and salinity ($R^2=0.29$, $p\text{-}$
255 $\text{value}=0.053$) is better compared to that between Mg/Ca and salinity, but remains relatively
256 weak. Nevertheless, recalculated regressions of Mg/Ca, incorporating salinity, show an
257 improvement of the correlation with temperature, best fit:

$$258$$
$$259 \quad \text{Mg/Ca} = \exp((-5.02 \pm 2) + (0.09 \pm 0.009) * T + (0.11 \pm 0.05) * S),$$
$$260 \quad R^2 = 0.91 \quad \text{pvalue} = 5e-06$$

261
262 This result is in good agreement with the recent study of Gray and Evans (2019), who reported
263 the minor Mg/Ca sensitivity of *Trilobatus sacculifer* to salinity ($3.6 \pm 0.01\%$ increase per
264 salinity unit) and described, based on previously published culture experiments' data (Dueñas-
265 Bohórquez et al., 2009; Hönisch et al., 2013; Kisakürek et al., 2008; Lea et al., 1999; Nürnberg
266 et al., 1996), a similar fit allowing to assess the sensitivity of foraminiferal Mg/Ca of *T.*
267 *sacculifer* to temperature and salinity combined.

$$268 \quad \text{Mg/Ca} = \exp(0.054(S-35) + 0.062T - 0.24) \quad \text{RSE: } 0.51 \quad \text{Gray and Evans (2019)}$$

269 Applying the equation of Gray and Evans (2019), to our data, leads to a correlation of 0.90,
270 which is identical than our findings. In order to further compare both equations, Mg/Ca values
271 from our study were used to reconstruct temperature and salinity using the fit established per
272 Gray and Evans (2019), versus reconstructed temperature and salinity using our fit. The
273 observed R^2 are then 0.99 and 0.48 for temperature and salinity, respectively. We can conclude,
274 that if the equation of Gray and Evans (2019), is in perfect agreement with our equation with
275 regards to the temperature parameter, this is not the case for salinity, which shows a strong
276 difference between the two equations, most probably explained by the weak correlation of
277 Mg/Ca to salinity in our data. Subsequently, the Bayesian model of Tierney et al. (2019)

278 considering the group-specific core-top model for *T. sacculifer* was applied to our data. In that
279 aim, Ω^{-2} and pH, were calculated using Alk and DIC data presented in table 1. Because
280 foraminifera in our studies were not submitted to cleaning protocol with a reductive step, the
281 clean parameter was set to 0. It led to the following correlation:

$$282 \quad \text{Mg/Ca} = \exp(-11.66 + 0.06 * T - 0.21 \Omega^{-2} + 1.40 \text{pH}) \quad R^2 = 0.82$$

283 Here we can conclude, that despite the difference in sampling strategy and samples
284 geographical distribution, our regression models are in line with the previous work of Gray and
285 Evans (2019) and Tierney et al. (2019).

286 **3.2. Stable isotopes concentration**

287 The $\delta^{18}\text{O}$ (PDB) values of the tests ($\delta^{18}\text{Oc}$) and of the seawater ($\delta^{18}\text{Ow}$) vary from -0.70 to -
288 2.98‰ and from 0.74 to 1.25‰, respectively (Tab. 1 and 2). The relationship between
289 temperature and the foraminiferal $\delta^{18}\text{O}$ (expressed as a difference to the $\delta^{18}\text{Ow}$ of the ambient
290 seawater) was estimated with a linear least squares regression:

$$291 \quad T = (12.08 \pm 1.46) - (4.73 \pm 0.51) * (\delta^{18}\text{Oc} - \delta^{18}\text{Ow}) [\text{‰}]; R^2 = 0.88 \quad (\text{equation 4})$$

292
293 The oxygen isotope fractionation ($\delta^{18}\text{Oc} - \delta^{18}\text{Ow}$) shows a strong correlation with *in situ* surface
294 water temperature (linear increase of 0.17‰/°C).
295

296 297 **3.3. Comparison with previously established *T. sacculifer* temperature reconstruction** 298 **equations**

299 As mentioned above, average juvenile and pre-adult *T. sacculifer* specimen only spend between
300 9 to 10 days in surface waters. Therefore, measured *in situ* temperature is representative of the
301 calcification temperatures. This is supported by the strong correlation between measured
302 temperature and $\delta^{18}\text{O}$ analyses ($R^2=0.90$, equation 4), and measured temperature vs. Mg/Ca,
303 ($R^2=0.87$, equation 1). Nevertheless, diurnal variations in temperatures cannot be discarded and
304 may induce a slight offset between measured average temperature and mean calcification
305 temperature.

306
307 For comparison, three Mg/Ca temperature calibrations for *T. sacculifer* were considered in this
308 manuscript. The equation of Nürnberg et al. (1996) based on laboratory cultures, (2) the
309 equation established by Anand et al. (2003) based on sediment trap samples and (3) the equation

310 derived by Regenberg et al. (2009) based on surface sediment samples of the Tropical Atlantic
311 Ocean. In each of these studies only *T. sacculifer* without SAC chamber were considered, (Tab.
312 3).

313 Similarly, in addition to equation 4 established in this study, three $\delta^{18}\text{O}$ based paleo-temperature
314 equations for *T. sacculifer* were used for comparison with our data set: (1) Erez and Luz, (1983)
315 and, (2) Spero et al. (2003), both based on cultured specimens, and (3) Mulitza et al. (2003)
316 based on surface water samples (Fig. 4; Tab. 3).

317

318 **3.4. Correlation between measured $\delta^{18}\text{O}$ /Salinity**

319 Salinity and the oxygen isotope composition of surface seawater were measured for 23 stations
320 located between 33°N and 27°S of the Eastern Atlantic Ocean (Tab. 4), including the thirteen
321 stations represented in figure 1, where foraminifera were sampled. The $\delta^{18}\text{O}_w$ -salinity
322 relationship (equation 5) is plotted in figure 5.

323

$$324 \quad \delta^{18}\text{O}_w = (0.171 \pm 0.04) * S - (4.93 \pm 1.66), R^2 = 0.38 \quad \text{(equation 5)}$$

325

326 For comparison, the $\delta^{18}\text{O}_w$ -salinity relationship for the tropical Atlantic Ocean calculated by
327 Paul et al. (1999) (from 25°S to 25°N) based on GEOSECS data, and by Regenberg et al.
328 (2009), based on data from Schmidt 1999 (30°N–30°S), are plotted in the same figure.
329 Temporal, geographical and depth differences in sampling, as well as analytical noise, are most
330 probably responsible for the observed variations.

331

332

4. DISCUSSION

333 **4.1. Intra-test variability**

334 The Mg/Ca and Sr/Ca composition of foraminiferal calcium carbonate was determined using
335 laser ablation ICP-MS of the final (F) chamber of size-selected specimen. Eggins et al., (2003)
336 report that the Mg/Ca composition of sequentially precipitated chambers of different species
337 (including *T. sacculifer*) are consistent with temperature changes following habitat migration
338 towards adult life-cycle stages. As described for *T. sacculifer* in the Red Sea (Bijma and
339 Hemleben, 1994), juvenile specimens (<100 μm) migrate to the surface, where they stay about
340 9-10 days, before descending to the reproductive depth (80m). The addition of GAM calcite
341 proceeds immediately prior to gamete release (Hamilton et al., 2008). The specimens
342 considered in this study were collected between 0 and 10 meters depth, and in agreement with
343 measurements on specimens from culture experiments (Dueñas-Bohórquez, 2009), Mg-rich

344 external surfaces (GAM calcite) were not observed in our samples. This indicates limited
345 vertical migration (see section 2.2. for reproduction cycle), reducing therewith potential
346 ontogenic vital effects responsible for inter-chamber elemental variations (Dueñas-Bohórquez,
347 2010) and, limited, if any, GAM calcite precipitation (Nürnberg et al., 1996). If the exact
348 calcification depth of the last chambers of our *T. sacculifer* specimen can still be questioned,
349 the lack of GAM-calcite, together with the strong correlation observed between measured
350 surface temperature vs. Mg/Ca-reconstructed temperature, support the idea that calcification of
351 the last chamber of our specimen occurred around 10 meters depth. It should be noted that Lessa
352 et al. (2020) recently confirmed that *T. sacculifer* calcifies in the upper 30 m. Because the
353 diameter of the laser beam used in this study was 80 μ m, it represents a reliable mean value of
354 elemental concentration of the last chamber wall, for every analysis of a single shell a full
355 ablation of the wall chamber was performed (until perforation was completed). For comparison,
356 results from traditional ICP-OES Mg/Ca analyses (Regenberg et al., 2009), electron microprobe
357 (Nurnberg et al., 1996) and laser ablation ICP-MS (this study) are plotted in figure 3a and
358 suggest comparable foraminiferal Mg/Ca ratios for *T. sacculifer* at similar temperatures.

359

360 **4.2. Incorporation of Sr into Mg/Ca-Temperature calibrations**

361 Combining Mg and Sr data to compute temperature was first suggested by Reichart et al. (2003)
362 for the aragonitic species *Hoeglundina elegans*. It has been demonstrated that variables other
363 than temperature, such as salinity and carbonate chemistry (possibly via their impact on growth
364 rate) are factors influencing Sr incorporation into calcite (e.g. Lea et al., 1999, Dueñas-
365 Bohórquez et al., 2009; Dissard et al., 2010a; Dissard et al., 2010b). The good correlation of
366 Sr/Ca with temperature in our results ($R^2=0.67$, p value= 5.e-04, Fig 2b), also suggests that
367 temperature exerts a major control on the amount of Sr incorporated into *T. sacculifer*' tests.
368 However, Sr/Ca concentration also shows a correlation with salinity ($R^2=0.29$, p-value=0.053),
369 which is not observed for Mg ($R^2=0.09$, p-value=0.32). Therefore, the incorporation of Sr into
370 the Mg-T reconstruction equation might improve temperature reconstruction by accounting for
371 the impact of salinity. It has recently been suggested that the Sr incorporation in benthic
372 foraminiferal tests is affected by their Mg contents (Mewes et al., 2015; Langer et al.; 2016).
373 However, as pointed out in Mewes et al., (2015), calcite's Mg/Ca needs to be over 30-50mmol
374 in order to noticeably affect Sr partitioning. There is no obvious reason to assume that
375 planktonic foraminifera should have a different Mg/Ca threshold. Therefore, with a
376 concentration between 2 to 6 mmol/mol (Sadekov et al., 2009), the observed variation in Sr
377 concentration in *T. sacculifer*' tests can be safely considered to be independent of the Mg/Ca

378 concentrations. Hence, other environmental parameters such as temperature, salinity and/or
379 carbonate chemistry, potentially via an impact on calcification rates, must control Sr/Ca values.

380

381 The standard deviation of measured temperatures versus reconstructed temperature was
382 calculated for each of the three Mg-temperature equations established in this study. For
383 equation (1), based on Mg/Ca only, SD= 1.37, for equation (3), based on both Mg/Ca and Sr/Ca,
384 SD=0.98, and for equation (4), based on Mg/Ca ratio and salinity, SD=1.03. Incorporation of
385 Sr into the Mg-Temperature reconstruction equation resulted in the standard deviation the
386 closest to 1 (SD=0.98), indicating that this statistically improved reconstructions possibly by
387 attenuating the salinity effect as well as potentially other environmental parameters such as
388 variations in carbonate chemistry or the effect of temperature itself. Therefore, the combination
389 of Mg/Ca and Sr/Ca should be considered to improve temperature reconstructions (Tab. 3). For
390 the remainder of this discussion, and in order to compare our data with previously established
391 calibrations for *T. sacculifer*, the equation based on Mg/Ca alone (equation 1) will be
392 considered.

393

394 **4.3 Comparison with previous *T. sacculifer* Mg/Ca-Temperature calibrations.**

395 Mg/Ca ratios measured on *T. sacculifer* from our study show a strong correlation with measured
396 surface water temperature ($R^2=0.86$, p value= $2.9e-06$) (Fig. 2a), increasing exponentially by
397 8.3% per °C. The relation with temperature (equation 1) is comparable to the one published by
398 Nürnberg et al., (1996) and within the standard error of the calibration (Fig. 3a). This implies
399 that the temperature controlled-Mg incorporation into *T. sacculifer* tests is similar under culture
400 conditions as it is in natural surface waters. The equation established by Duenas-Bohorquez et
401 al., (2010) based on *T. sacculifer* specimen from culture experiments integrates ontogenetic
402 (chamber stage) effects. Even though incorporating the ontogenetic impact may improve
403 temperature reconstructions based on Mg/Ca ratios, this is not routinely done for paleo-
404 temperature reconstruction using *T. sacculifer*. Therefore, the equation of Nürnberg et al.,
405 (1996) is used in our study for comparison of various reconstruction scenarios.

406 A comparable regression (similar slope) has been established for *T. sacculifer* from tropical
407 Atlantic and Caribbean surface sediment samples by Regenberg et al. (2009) (Fig 3a). This
408 regression predicts Mg concentrations that are about 0.15 mmol/mol higher compared to our
409 study. Because the Mg-T calibration from Regenberg et al. (2009) is based on sediment-surface
410 samples, Mg concentrations were correlated with reconstructed mean annual temperatures. This
411 potentially leads to an over or under-estimation of temperatures depending on the seasonality

412 of the growth period and might explain the observed difference between the two regressions.
413 Due to sample limitation, we analysed foraminifera from a wider size fraction (230 μ m to
414 500 μ m), compared to Regenberg et al. (2009) (355-400 μ m), introducing an additional bias
415 between the two datasets (Duenas-Bohorquez et al., 2010; Friedrich et al., 2012). Finally,
416 Regenberg et al. (2009), compiled data of samples from the tropical Atlantic and Caribbean
417 Ocean, while we collected samples from the Eastern tropical Atlantic. All of these potential
418 biases can easily explain the small discrepancy observed between our regression and the one
419 from Regenberg et al., (2009). Interestingly, Jentzen et al., (2018), were able to compare Mg/Ca
420 ratios measured on *T. sacculifer* from both surface sediment samples of the Caribbean sea and
421 specimen sampled with a plankton net nearby. They observed a similar systematic increased
422 Mg/Ca ratio in fossils tests of *T. sacculifer* (+0.7 mmol/mol-1) compared to living specimens,
423 arguing that different seasonal signals were responsible for the observed difference. However,
424 it is interesting to note that the Mg/Ca differences observed between living *T. sacculifer* (e.g.
425 this study and Jentzen et al., 2018) and fossils specimens (e.g. Regenberg et al., 2009 and
426 Jentzen et al., 2018) could also be explained by the presence of GAM calcite on *T. sacculifer*
427 from sediment samples, as GAM calcite is enriched with Mg compared to pre-gametogenetic
428 calcite precipitated at the same temperature (Nurnberg et al., 1996). If Jentzen et al., (2018) and
429 Regenberg et al. (2009) do not describe the presence or absence of GAM calcite on *T. sacculifer*
430 specimens analysed in their studies, a study on the population dynamics of *T. sacculifer* from
431 the central Red Sea Bijma and Hemleben (1990) concluded that the rate of gametogenesis
432 increased exponentially between 300 and 400 μ m to reach a maximum of more than 80% at
433 355 μ m (sieve size =500 μ m real test length). It can therefore safely be assumed that the Mg/Ca
434 difference between living specimens from the plankton and empty shells from the sediment is
435 due to GAM calcite.

436 The Mg-Temp data obtained by Jentzen et al., (2018) is however, in good agreement with the
437 equation established by Regenberg et al., (2009), and will therefore not be considered separately
438 in this study. The overall strong similarity observed between our regression and the one from
439 Regenberg et al. (2009), indicates nevertheless that Mg-temp calibrations established on *T.*
440 *sacculifer* specimen from plankton tow, can be applied to *T. sacculifer* (without Sac) from the
441 surface-sediment, even if these applications have to be considered with care and only on
442 sediment samples showing no sign of dissolution.

443 In contrast, the equation of Anand et al., (2003) based on sediment trap samples, is appreciably
444 different (Fig. 3b). This may be due to: (1) difference in cleaning and analytical procedures, (2)
445 addition of GAM calcite at greater depth and (3) uncertainty in estimated temperature, indeed,

446 as mentioned in Gray et al., (2019): “Note the calibration line of Dekens et al. (2002) and Anand
447 et al. (2003) does not fit the data of Anand et al. (2003) when climatological temperature, rather
448 than the $\delta^{18}\text{O}_{\text{calcite}} - \delta^{18}\text{O}_{\text{water}}$ temperature, is used. As shown by Gray et al., (2019), we show
449 the calibrations of Anand et al (2003) are inaccurate due to seasonal changes in the $\delta^{18}\text{O}$ of sea
450 water at that site.

451 Anand et al., (2003) fixed the intercept of the exponential regression for *T. sacculifer* to the
452 value obtained for a multispecies regression and subsequently recalculated for each species the
453 pre-exponential coefficients. Using this approach their new equation for *T. sacculifer* is:
454 $\text{Mg}/\text{Ca} = 0.35 \exp(0.09 \cdot T)$, which is identical to Nürnberg et al., (1996) and equation 1 from
455 our study. Still, this implicitly assumes a common temperature dependence exists for all
456 species, which is not realistic. To avoid *a priori* assumptions only the primary equation of
457 Anand et al., (2003) (see Tab. 3) is considered in this study.

458

459 **4.4. Comparison with previous $\delta^{18}\text{O}$ -Temperature calibrations.**

460 As for Mg/Ca, the oxygen isotope composition also shows a strong correlation with measured
461 surface water temperature ($R^2=0.90$). The *T. sacculifer* $\delta^{18}\text{O}$ -temperature equation of Spero et
462 al., (2003), based on a culture experiment, is very similar to equation 4 in our study. However,
463 sensitivity (slope) differs within the uncertainties calculated for equation 4. As no uncertainties
464 are given for the Spero et al., (2003) equation, it is difficult to determine whether these
465 equations are statistically different or not. In contrast, the equation of Mulitza et al., (2003), has
466 a similar slope (within uncertainties) but a higher intercept (Fig. 4a). The equation of Erez and
467 Luz, (1983) differs considerably from equation 4, for both slope and intercept parameters.
468 Bemis et al., (1998) suggested a bias in the calibration due to uncontrolled carbonate chemistry
469 during the experiments of Erez and Luz (1983) (a decrease in pH, e.g. due to bacterial growth
470 in the culture medium or to a higher CO_2 concentration in the lab (air conditioners, numerous
471 people working in the same room etc), would quickly lead to an increase in $\delta^{18}\text{O}$ of culture-
472 grown foraminifera). This could explain the observed effect between our study (equation 4) and
473 the calibration from Erez and Luz (1983). Although the equation of Mulitza et al., (2003) is
474 also based on *T. sacculifer* collected from surface waters, their equation is significantly different
475 from equation (4). This deviation could possibly be due to a difference in size fractions
476 considered in the two studies (230 to 500 μm , and 150 to 700 μm for this study and Mulitza et
477 al., (2003), respectively). Berger et al. (1979), already reported that large *T. sacculifer* tests are
478 enriched in $\delta^{18}\text{O}$ relative to smaller ones (variation of 0.5‰ between 177 and 590 μm).

479 Similarly, in culture experiments, larger shells of *Globigerina bulloides* are isotopically heavier
480 relative to smaller specimens (variation of approximately 0.3‰ between 300 to 415µm,
481 Bemis et al., 1998). Jentzen et al., (2018) reported that: ‘Enrichment of the heavier ¹⁸O isotope
482 in living specimens below the mixed layer and in fossil tests is clearly related to lowered in situ
483 temperatures and gametogenic calcification’. Gametogenic calcite has been shown to enrich
484 δ¹⁸O signatures by about 1.0-1.4‰ relative to pregametogenic *T. sacculifer* (Wyceh et al.,
485 2018). Finally, variation in light intensity (e.g. due to different sampling period and/or sampling
486 location), may have influenced the δ¹⁸O composition via an impact on symbiont activity (Spero
487 and DeNiro, 1987). Bemis et al. (1998) demonstrated that in seawater with ambient [CO₃²⁻],
488 *Orbulina universa* shells grown under high light level (> 380 µEinst m⁻² s⁻¹) are depleted in ¹⁸O
489 by on average 0.33‰ relative to specimens grown under low light levels (20-30 µEinst m⁻² s⁻¹).
490 The different correlation between δ¹⁸O and temperature reported by Mulitza et al., (2003) may
491 be caused by size fraction differences, different sampling time, light intensity, differences in
492 calcification depth or hydrography, or a combination of factors. These are all potential biases
493 that could explain the steeper intercept observed by Mulitza et al., (2003) relative to our study.

494

495 **5. Reconstructions**

496 A few scenarios are considered in the following section, in which one, two or three proxy
497 equations are combined to solve for salinity.

498

499 Three Mg/Ca-paleo-temperature equations (Nürnberg et al., 1996; Regenberg et al., 2009; and
500 Anand et al., 2003) were used to compare “reconstructed” temperatures to the known *in situ*
501 surface waters temperatures. The mean foraminiferal Mg/Ca ratio measured at each of our
502 stations was inserted into each of the three equation and solved for temperature (Fig. 3b.). The
503 linear regression of reconstructed temperatures based on Nürnberg et al. (1996) overlaps almost
504 perfectly with the theoretical best fit. This confirms that calibrations based on culture
505 experiments (the primary geochemical signal recorded in the tests) are very well-suited for
506 reconstructing surface water temperature. The regression from Regenberg et al., (2009)
507 reconstructed surface temperature that are too warm. This is in agreement with the fact that the
508 Mg/Ca ratio from surface sediment foraminifera are slightly higher than for living specimen
509 (Jentzen et al. 2018). The offset increases with decreasing temperature (0.5°C and 1.5°C
510 respectively at 30°C and 16°C). Finally, the reconstructed temperature using the equation from
511 Anand et al. (2003), shows a strong systematic offset. Because the equation of Nürnberg et al.,
512 (1996) matched our measured temperatures almost perfectly, their equation will be used to

513 analyse further reconstruction. Still, we acknowledge that downcore reconstructions will
 514 inevitably also involve GAM calcite and hence other calibrations established using specimens
 515 collected deeper in the water column or in the sediment should be better suitable. Similarly,
 516 three $\delta^{18}\text{O}$ -paleo temperature equations (Erez and Luz, 1983; Mulitza et al., 2003; Spero et al.,
 517 2003) were tested to reconstruct $\delta^{18}\text{Oc}$ - $\delta^{18}\text{Ow}$. The equation of Erez and Luz, (1983), shows a
 518 significant systematic overestimation of $\delta^{18}\text{Oc}$ - $\delta^{18}\text{Ow}$, and will therefore not be considered any
 519 further. Measured surface water temperatures at our 13 stations were inserted into the equations
 520 of Mulitza et al., (2003) and Spero et al., (2003) to derive $\delta^{18}\text{Oc}$ - $\delta^{18}\text{Ow}$ (Fig. 4). The $\delta^{18}\text{Oc}$ -
 521 $\delta^{18}\text{Ow}$ reconstructions based on the equation of Mulitza et al. (2003) and Spero et al. (2003),
 522 are both slightly more positive, than the theoretical best fit. In order to test the robustness of
 523 $\delta^{18}\text{Ow}$ reconstructions from paleoceanographic literature (e.g. Nürnberg and Groeneveld, 2006;
 524 Bahr et al., 2011), we use the reconstructed temperatures based on the Mg/Ca-paleo-
 525 temperature equation from Nürnberg et al., (1996) to predict $\delta^{18}\text{Ow}$ using measured $\delta^{18}\text{Oc}$ and
 526 the equations from Mulitza et al., (2003) and Spero et al. (2003). The reconstructed $\delta^{18}\text{Oc}$ -
 527 $\delta^{18}\text{Ow}$ from inserting the Mg/Ca temperature into these equations is slightly overestimated
 528 (0.5‰), but the offsets remain small enough to consider these as reasonable reconstructions.

529

530 When reconstructing $\delta^{18}\text{Ow}$ by inserting the Mg/Ca temperature and measured $\delta^{18}\text{Oc}$ in both
 531 equations, the correlation coefficients of the linear regressions are weak ($R^2 = 0.19$ and 0.13 for
 532 Spero et al., 2003 and Mulitza et al., 2003, respectively) demonstrating that the reconstructed
 533 $\delta^{18}\text{Ow}$ is not very reliable, therefore no reconstruction of salinity using these equations will be
 534 further tested in this manuscript.

535

536 Nevertheless, to test the robustness of theoretical and empirical salinity reconstructions, we
 537 have the perfect data set at hand, as every parameter is known from *in situ* measurement or
 538 sampling. We will use the equations 1, 4 and 5 established in this study and presented in table
 539 3, for demonstration purposes.

540

$$541 \quad \text{Mg/Ca} = ae^{bT} \quad \text{Eq. 1}$$

542 with $a=0.42(\pm 0.13)$ and $b= 0.083(\pm 0.001)$

543

$$544 \quad T = c + d(\delta^{18}\text{Oc} - \delta^{18}\text{Ow}) \quad \text{Eq. 4}$$

545 with $c=12.08(\pm 1.46)$ and $d=-4.73(\pm 0.51)$

546

547
$$\delta^{18}O_w = eS + f \quad \text{Eq. 5}$$

548 with $e=0.171(\pm 0.04)$ and $f = -4.93(\pm 1.66)$

549 Classically, from those equations it is possible to extract variables estimated from the
550 observation Mg/Ca and $\delta^{18}Oc$ through the equations:

551
$$\hat{T} = \frac{1}{b} (\log (Mg/Ca) - \log(a)) \quad \text{Eq.1'}$$

552
$$\delta^{18}\widehat{O}_w = \delta^{18}Oc - \frac{1}{d} (\hat{T} - c) \quad \text{Eq. 4'}$$

553
$$\hat{S} = \frac{1}{e} (\delta^{18}\widehat{O}_w - f) \quad \text{Eq. 5'}$$

554

555

556 Given that \hat{T} is estimated from the fit from Eq. 1' (fig. 3a) and $\delta^{18}\widehat{O}_w$ is estimated from Eq. 4',
557 \hat{S} is finally calculated from Eq. 5' (figure 5). Hence, the error in \hat{S} is an accumulation of errors
558 from successive fits. In this study the standard deviation of the fit between \hat{S} and the measured
559 salinity for the 13 stations is ± 2.49 and the R^2 is 0.33 (p-value 0.04) (Fig. 6a and b). In
560 conclusion, even the best possible salinity reconstruction based on locally calibrated equations
561 1, 4 and 5 from the present study only allows salinity reconstructions with a precision of ± 2.49 .
562 In the modern Atlantic Ocean, and based on recent sea surface salinity estimation (Vinogradova
563 et al., 2019), such a variability would not allow to distinguish water masses between 60°N to
564 60°S. Similarly, on a temporal timescale, given the regional salinity variations expected in most
565 of the ocean over glacial-interglacial cycles is less than $\pm 1, 2\sigma$ (Gray and Evans, 2019), such an
566 incertitude on salinity reconstruction would not even allow to distinguish modern *versus* last
567 glacial maximum water masses.

568

569 In the following steps, we quantify the error propagation more precisely. In simple cases, error
570 accumulation in an equation can be assessed by calculating the partial derivatives and by
571 propagating the uncertainties of the equation with respect to the predictors (Clifford, 1973).
572 However, for complex functions the calculation of partial derivatives can be tedious. Here, error
573 propagation related to \hat{S} was computed by a Monte Carlo simulation, which is simple to
574 implement (Anderson, 1976), and in line with the method applied by Thirumalai et al., (2019)
575 on sediment samples *G. Ruber* (W) specimen. It is important to note that the propagated error
576 with a reconstructed salinity is a combination of fitting errors and errors associated with
577 measurement inaccuracies (Mg/Ca and $\delta^{18}Oc$). First, we will only consider the error related to
578 the fitting procedure, (Eq. 1', 4' and 5', assuming that variables (i.e. the data) are perfectly

579 known without uncertainties). For example, the fitting error related to Eq. 4' is computed by
 580 fitting $\delta^{18}\text{O}_w$ from measured $\delta^{18}\text{O}_c$ and measured Temperature, i.e. the data are known and
 581 not approximated. This is done by adding random Gaussian noise, with standard deviation
 582 corresponding to the RMSE (Root Mean Square error) of each fit (respectively 1.32°C for
 583 Eq.1', 0.15‰ for Eq. 4' and 0.55 for Eq. 5'). The resulting standard deviation error for the
 584 reconstructed Salinity based on 10000 fits following the Monte-Carlo approach amounted to
 585 ± 1.69 (each fit using sampling from random distributions defined above). Hence, ± 1.69 is the
 586 smallest possible error for salinity reconstructions, using the three steps above, only due to its
 587 mathematics. We can also estimate the error propagation at each step: $\hat{T} \pm 1.32^\circ\text{C}$ (Eq.1'),
 588 $\widehat{\delta^{18}\text{O}_w} \pm 0.45\text{‰}$ (Eq.4') and $\hat{S} \pm 1.69$ (Eq.5'). Now we will include the uncertainties related to
 589 estimating the variables using proxy data. Hereto, some Gaussian noises simulating the
 590 uncertainties of measured variables (Mg/Ca and $\delta^{18}\text{O}_c$) were introduced with standard
 591 deviations taken from Table 2. The resulting standard deviation error increased to ± 2.65 .
 592 Therefore, it can be concluded that statistically speaking, $\widehat{\delta^{18}\text{O}_w}$ cannot be reconstructed to a
 593 precision better than $\pm 0.45\text{‰}$, while salinity cannot be reconstructed to a precision better than
 594 ± 1.69 (fitting errors only) and, in reality hardly better than ± 2.65 (full to error propagation).

595
 596 Finally, to complete this analysis, a direct linear fit to estimate salinity using $\exp(-\delta^{18}\text{O}_c)$
 597 and Mg/Ca was performed and led to an error of ± 0.26 and a $R^2 = 0.82$ (p-value 2.10^{-4}):

$$599 \quad \hat{S} = -0.16(\pm 0.02) e^{-\delta^{18}\text{O}_c} + 0.28(\pm 0.1) \frac{\text{Mg}}{\text{Ca}} + 35.80(\pm 0.33) \quad (R^2=0.81, \text{p-value} \approx 2.10^{-4}) \quad \text{Eq. 6}$$

600
 601 This demonstrates that the direct reconstruction using the exact same variables as those initially
 602 measured (Mg/Ca and $\delta^{18}\text{O}_c$), led to a much better estimation of salinity than the successive
 603 reconstruction.

606 **6. Implications**

607 We analyzed shell Mg/Ca and Sr/Ca ratios, and $\delta^{18}\text{O}$ in *T. sacculifer* collected from surface
 608 water along a North-South transect of the Eastern Tropical Atlantic Ocean. We find a strong
 609 correlation between Mg/Ca ratios and surface water temperature, confirming the robustness of
 610 surface water temperature reconstructions based on *T. sacculifer* Mg/Ca.

611 Insertion of the Sr/Ca ratio into the paleo-temperature equation improves the temperature
612 reconstruction. We established a new calibration for a paleo-temperature equation based on
613 Mg/Ca and Sr/Ca ratios for live *T. sacculifer* collected from surface water:

614

$$615 \quad T = (-27 \pm 15) + (8 \pm 1) * \ln(\text{Mg/Ca}) + (28 \pm 11) * \text{Sr/Ca}$$

616

617 Scenarios were tested using previously published reconstructions. Results were compared to
618 reconstructions performed using local calibrations established in this study and therefore
619 supposed to represent the best possible calibration for this data set:

620 (1) Mg/Ca ratios measured in *T. sacculifer* specimens collected in surface water allow accurate
621 reconstruction of surface water temperature.

622 (2) $\delta^{18}\text{O}_w$ can be reconstructed with an uncertainty of $\pm 0.45\%$. Such $\delta^{18}\text{O}_w$ reconstructions
623 remain a helpful tool for paleo-reconstructions considering the global range of variation of
624 surface $\delta^{18}\text{O}_w$ (from about -7 to 2‰, LeGrande and Schmidt 2006;).

625

626 (3) In contrast, the best possible salinity reconstruction based on locally calibrated equations 1,
627 4 and 5 from the present study, only allowed reconstruction with an uncertainty of ± 2.49 . Such
628 an uncertainty renders these reconstructions meaningless and does not allow for viable
629 (paleo)salinity data.

630 This is confirmed by a Monte Carlo simulation, applied to test successive reconstructions in an
631 'ideal case', where explanatory variables are known. This simulation shows that from a pure
632 statistical point of view, successive reconstructions involving Mg/Ca and $\delta^{18}\text{O}_c$ preclude
633 salinity reconstruction with a precision better than ± 1.69 and hardly better than ± 2.65 , due to
634 error propagation.

635 Nevertheless, a direct linear fit to reconstruct salinity based on the same measured variables
636 (Mg/Ca and $\delta^{18}\text{O}_c$) was established (Eq. 6) and presented in table 3. This direct reconstruction
637 of salinity should lead to a much better estimation of salinity (± 0.26) than the successive
638 reconstructions.

639

640 **ACKNOWLEDGEMENTS**

641 We thank captain and crew of the Polarstern cruise ANT XXIII/1, (Bremerhaven-Cape Town)
642 who have been of great support during this unforgettable experience. We are grateful to Susann
643 Grobe of the Marine Biogeochemistry group of the IFM-GEOMAR (Germany) for measuring
644 DIC and ALK of water samples. We thank Arnold Van Dijk of the Department of Earth

645 Sciences-Geochemistry of the University of Utrecht (The Netherlands) for measuring oxygen
646 isotope composition of water and foraminifera. We are thankful to Gijs Nobbe and Dr. Paul
647 Mason for their support with LA-ICP-MS analyses. We would like to thank Beate Mueller
648 (formaly Hollmann) for her technical support when handling foraminifera, and Dr. Gernot
649 Nehrke, Dr. Stephan Mulitza, and Dr. Aurore Receveur for improving earlier versions of the
650 manuscript. We thank Prof. Dieter Wolf Gladrow for his support during the initial draft of this
651 manuscript. This work was supported by the German research foundation (DFG) under grant
652 no. BI 432/4-2 ("PaleoSalt"), and by the European Science Foundation (ESF) under the
653 EUROCORES Programme EuroCLIMATE through contract No. ERAS-CT-2003-980409 of
654 the European Commission, DG Research, FP6. Gert-Jan Reichart acknowledges funding from
655 the program of the Netherlands Earth System Science Centre (NESSC), by the Ministry of
656 Education, Culture and Science (OCW; Grant 024.002.001).

657

658 **AUTHORS CONTRIBUTION**

659 J.B., G-J.R., and D.D., designed the research and initiated the original project. D.D. completed
660 the foraminifera sampling, sample processing, data analysis and served as primary author on
661 this manuscript. G-J.R. assisted D.D. in LA-ICPMS analyses. S.F. assisted D.D. in statistical
662 treatments associated with data interpretations. M.M. and CM completed the Monte Carlo
663 simulation. All of the authors assisted in interpretation, editing, discussed the results and wrote
664 the manuscript.

665

666

REFERENCES

667

668 Anand P, Elderfield H, and Conte MH, 2003. Calibration of Mg/Ca thermometry in planktonic
669 foraminifera from a sediment trap time series. *Paleoceanography* 18, 15. DOI:
670 10.1029/2002PA000846.

671 Anderson GM, 1976. Error propagation by the Monte Carlo method in geochemical
672 calculations, *Geochimica et Cosmochimica Acta*, Volume 40, Issue 12, 1976, Pages
673 1533-1538. DOI: 10.1016/0016-7037(76)90092-2.

674 Bahr A, Nurnberg D, Schonfeld J, Garde-Schonberg D, 2011. Hydrological variability in
675 Florida Straits during Marine Isotope Stage 5 cold events. *Paleoceanography* 26,
676 PA2214. DOI: 10.1029/2010PA002015.

- 677 Bé AWH, Spero HJ, and Anderson OR, 1982. The effects of symbiont elimination and
678 reinfection on the life processes of the planktonic foraminifer, *Globigerinoides*
679 *sacculifer*. *Mar. Biol.*, 70: 73-86. DOI: 10.1007/bf00397298.
- 680 Berger WH, 1979. Stable isotopes in foraminifera In: Lipps JH, Berger WH, Buzas MA,
681 Douglas RG, and Ross CA, Editors, *Foraminiferal Ecology and Paleocology, SEPM*
682 *Short Course vol. 6*, Society of Economic Paleontologists and Mineralogists, Houston,
683 Texas (1979), pp. 56–91. DOI:10.2110/scn.79.06.0156.
- 684 Bemis BE, Spero HJ, Bijma J, Lea DW, 1998. Reevaluation of the oxygen isotopic composition
685 of planktonic foraminifera: Experimental results and revised paleotemperature
686 equations. *Paleoceanography* 13(2): 150-160. DOI: 10.1029/98PA00070.
- 687 Bijma J, Faber WW, and Hemleben C, 1990. Temperature and Salinity Limits for Growth and
688 Survival of Some Planktonic Foraminifers in Laboratory Cultures. *Journal of*
689 *Foraminiferal Research* 20, 95-116. DOI: 10.2113/gsjfr.20.2.95.
- 690 Bijma J and Hemleben C, 1993. Population-dynamics of the planktic foraminifera
691 *Globigerinoides-sacculifer* (Brady) from the central red-sea. *Deep-Sea Research Part*
692 *I-Oceanographic Research Papers* 41: 485-510. DOI: 10.1016/0967-0637(94)90092-2.
- 693 Bijma J, Hemleben C, and Wellnitz K, 1994. Lunar-Influenced Carbonate Flux of the Planktic
694 Foraminifer *Globigerinoides-Sacculifer* (Brady) from the Central Red-Sea. *Deep-Sea*
695 *Research Part I-Oceanographic Research Papers* 41, 511-530. DOI: 10.1016/0967-
696 0637(94)90093-0.
- 697 Cleroux C, Cortijo E, Anand P, Labeyrie L, Bassinot F, Caillon N, Duplessy JC, 2008. Mg/Ca
698 and Sr/Ca ratios in planktonic foraminifera: Proxies for upper water column temperature
699 reconstruction. *Paleoceanography* 23. DOI: 10.1029/2007PA001505.
- 700 Clifford A, 1973. Multivariate error analysis: a handbook of error propagation and calculation
701 in many-parameter systems. *John Wiley and Sons*. ISBN 978-0470160558.
- 702 Dissard D, Nehrke G, Reichart GJ, Bijma J. 2010a. The impact of salinity on the Mg/Ca and
703 Sr/Ca ratio in the benthic foraminifera *Ammonia tepida*: Results from culture
704 experiments. *Geochimica Et Cosmochimica Acta* 74: 928-940.
705 DOI: 10.1016/j.gca.2009.10.040.
- 706 Dissard D, Nehrke G, Reichart GJ, Bijma J. 2010b. Impact of seawater pCO₂ on calcification
707 and Mg/Ca and Sr/Ca ratios in benthic foraminifera calcite: results from culturing
708 experiments with *Ammonia tepida*. *Biogeosciences* 7: 81-93. DOI: 10.5194/bg-7-81-
709 2010.

710 Dissard D, Nehrke G, Reichart GJ, Nouet J, Bijma J. 2009. Effect of the fluorescent indicator
711 calcein on Mg and Sr incorporation into foraminiferal calcite. *Geochemistry Geophysics*
712 *Geosystems* 10, Q11001 DOI:10.1029/2009GC002417.

713 Dueñas-Bohórquez A, da Rocha RE, Kuroyanagi A, Bijma J, Reichart GJ. 2009. Effect of
714 salinity and seawater calcite saturation state on Mg and Sr incorporation in cultured
715 planktonic foraminifera. *Marine Micropaleontology* 73: 178-189.
716 DOI: 10.1016/j.marmicro.2009.09.002.

717 Dueñas-Bohórquez A, da Rocha RE, Kuroyanagi A, de Nooijer LJ, Bijma J, Reichart GJ. 2009.
718 Interindividual variability and ontogenetic effects on Mg and Sr incorporation in the
719 planktonic foraminifer *Globigerinoides sacculifer*. *Geochemica and cosmochemica*
720 *acta* 75: 520-532. DOI: 10.1016/j.gca.2010.10.006.

721 Eggins S, De Deckker P, Marshall J. 2003. Mg/Ca variation in planktonic foraminifera tests:
722 implications for reconstructing palaeo-seawater temperature and habitat migration.
723 *Earth and Planetary Science Letters* 212: 291-306. DOI: 10.1016/S0012-
724 821X(03)00283-8.

725 Elderfield H and Ganssen G, 2000. Past temperature and delta O¹⁸ of surface ocean waters
726 inferred from foraminiferal Mg/Ca ratios. *Nature* 405, 442-445. DOI:
727 10.1038/35013033.

728 Emiliani C, 1954. Depth habitats of some species of pelagic foraminifera as indicated by
729 oxygen isotope ratios. *Amer J Sci*, v. 252, p. 149-158. DOI: 10.2475/ajs.252.3.149.

730 Epstein S, Buchsbaum R, Lowenstam HA, and Urey CH, 1953. Revised carbonate-water
731 isotopic temperature scale. *Geological Society of American Bulletin* 64, pp. 1315–1326.
732 DOI: 10.1130/0016-7606(1953)64[1315:RCITS]2.0.CO;2.

733 Erez J, and Luz B. 1983. Experimental Paleotemperature Equation for Planktonic-Foraminifera.
734 *Geochimica Et Cosmochimica Acta* 47, 1025-1031. DOI: 10.1016/0016-
735 7037(83)90232-6.

736 Friedrich O, Schiebel R, Wilson PA, Weldeab S, Beer CJ, Cooper MJ, Fiebig J. 2012. Influence
737 of test size, water depth, and ecology on Mg/Ca, Sr/Ca, δ¹⁸O and δ¹³C in nine modern
738 species of planktic foraminifers. *Earth and Planetary Science Letters* 319-320: 133-
739 145. DOI: 10.1016/j.epsl.2011.12.002.

740 Gaffey SJ and Bronnimann CE, 1993. Effects of Bleaching on Organic and Mineral Phases in
741 Biogenic Carbonates. *Journal of Sedimentary Petrology* 63, 752-754.
742 DOI: 10.1029/2018GC007575.

743 Gray WR, Rae JWB, Wills RCJ, Shevenell AE, Taylor BJ, Burke A, Foster GL; Lear
744 CH (2018): Deglacial planktic foraminiferal boron isotope and Mg/Ca data from
745 sediment core MD01-2416 in the western North Pacific Ocean. *Nature Geoscience*, Vol.
746 11, No. 5, 05.2018, p. 340–344. DOI: 10.1594/PANGAEA.887381.

747 Gray WR and Evans D, 2019. Nonthermal influences on Mg/Ca in planktonic foraminifera: A
748 review of culture studies and application to the last glacial maximum.
749 *Paleoceanography and Paleoclimatology* 34, 306-315. DOI: 10.1029/2018PA003517.

750 Groeneveld J, Ho SL, Mackensen A, Mohtadi M, Laepple T. 2019. Deciphering the variability
751 in Mg/Ca and Oxygen Isotopes of individual foraminifera. *Paleoceanography and*
752 *Paleoclimatology* 34, 755-773. DOI: 10.1029/2018PA003533.

753 Hamilton CP, Spero HJ, Bijma J, Lea DW. 2008. Geochemical investigation of gametogenic
754 calcite addition in the planktonic foraminifera *Orbulina universa*. *Marine*
755 *Micropaleontology* 68: 256-267. DOI: 10.1016/j.marmicro.2008.04.003.

756 Hastings DW, Russell AD, and Emerson SR, 1998. Foraminiferal magnesium in
757 *Globeriginoides sacculifer* as a paleotemperature proxy. *Paleoceanography* 13, 161-
758 169. DOI: 10.1029/97PA03147.

759 Hemleben C, Spindler M and Anderson OR, 1989. Modern planktonic foraminifera, *Springer*
760 *Verlag, Berlin*, 363 p. ISBN 978-1-4612-3544-6.

761 Honisch B, Allen KA, Lea DW, Spero HJ, Eggins SM, Arbuszewski J, deMenocal P, Rosenthal
762 Y, Russell AD, Elderfield H. 2013. The influence of salinity on Mg/Ca in planktic
763 foraminifers- Evidence from cultures, core-top sediments and complementary $\delta^{18}\text{O}$.
764 *Geochimica et Cosmochimica Acta* 121: 196-213. DOI: 10.1016/j.gca.2013.07.028.

765 Hut G, 1987. Consultant's group meeting on stable isotope reference samples of geochemical
766 and hydrological investigations. *IAEA, Vienna*, p 42 Report to the Director General.
767 INIS-MF—10954.

768 Jentzen A, Nurnberg D, Hathorne EC and Schonfeld J, 2018. Mg/Ca and $\delta^{18}\text{O}$ in living planktic
769 foraminifers from the Caribbean, Gulf of Mexico and Florida Straits. *Biogeosciences*, 15,
770 7077-7095. DOI: 10.5194/bg-15-7077-2018.

771 Jochum KP, Weis U, Stoll B, Kuzmin D, Yang Q, Raczek I, Jacob DE, Stracke A, Birbaum K,
772 Frick DA, Gunther D, Enzweiler J, 2011. Determination of reference values for NIST
773 610-617 glasses following ISO guidelines. *Geostandards and Geoanalytical research*.
774 35, 397–429, 201. DOI: 10.1111/j.1751-908X.2011.00120.x.

775 Johnson KM, Wills KD, Butler DB, Johnson WK and Wong, CS, 1993. Coulometric Total
776 Carbon-Dioxide Analysis for Marine Studies - Maximizing the Performance of an

777 Automated Gas Extraction System and Coulometric Detector. *Marine Chemistry* 44,
778 167-187. DOI: 10.1016/0304-4203(93)90201-X.

779 Kisakurek B, Eisenhauer A, Bohm F, Garbe-Schonberg D, Erez J. 2008. Controls on shell
780 Mg/Ca and Sr/Ca in cultured planktonic foraminiferan, *Globigerinoides ruber* (white).
781 *Earth and Planetary Science Letters* 273: 260-269. DOI: 10.1016/j.epsl.2008.06.026.

782 Kontakiotis G, Mortyn GP, Antonarakou A, Drinia H, 2016. Assessing the reliability of
783 foraminiferal Mg/Ca thermometry by comparing field-samples and culture experiments:
784 a review. *Geological quarterly*, 2016, 60 (3): 547-560. DOI: 10.7306/gq.1272.

785 Langer G, Sadekov A, Thoms S, Keul N, Nehrke G, Mewes A, Greaves M, Misra S, Reichart
786 GJ, de Nooijer LJ, Bijma J, Elderfield H, 2016. Sr partitioning in the benthic
787 foraminifera *Ammonia aomoriensis* and *Amphistegina lessonii*. *Chemical Geology* 440
788 (2016) 306-312. DOI: 10.1016/j.chemgeo.2016.07.018.

789 Lea DW, Mashiotta TA, and Spero HJ, 1999. Controls on magnesium and strontium uptake in
790 planktonic foraminifera determined by live culturing. *Geochimica Et Cosmochimica*
791 *Acta* 63, 2369-2379. DOI: 10.1016/S0016-7037(99)00197-0.

792 Lear CH, Rosenthal Y, and Slowey N, 2002. Benthic foraminiferal Mg/Ca-paleothermometry:
793 A revised core-top calibration. *Geochimica Et Cosmochimica Acta* 66, 3375-3387.
794 DOI: 10.1016/S0016-7037(99)00197-0.

795 LeGrande AN and Schmidt GA, 2006. Global gridded data set of the oxygen isotopic
796 composition in seawater. *Geophys. Res. Lett.* 33, L12604. DOI:
797 10.1029/2006GL026011.

798 Lessa, D., Morard, R., Jonkers, L., Venancio, I. M., Reuter, R., Baumeister, A., Albuquerque,
799 A.L., Kucera, M. (2020). Distribution of planktonic foraminifera in the subtropical
800 South Atlantic: depth hierarchy of controlling factors. *Biogeosciences*, 17(16), 4313-
801 4342. doi:10.5194/bg-17-4313-2020.

802 Mewes A, Langer G, Reichart GJ, de Nooijer LJ, Nehrke G, Bijma J, 2015. The impact of Mg
803 contents on Sr partitioning in benthic foraminifers. *Chemical Geology* 412: 92-98.
804 DOI: 10.1016/j.chemgeo.2015.06.026.

805 Mintrop L, Perez FF, Gonzalez-Davila M, Santana-Casiano MJ, and Kortzinger A, 2000.
806 Alkalinity determination by potentiometry: Intercalibration using three different
807 methods. *Ciencias Marinas* 26, 23-37. DOI: 10.7773/cm.v26i1.573.

808 Mulitza S, Boltovskoy D, Donner B, Meggers H, Paul A, and Wefer G. 2003. Temperature:
809 delta O¹⁸ relationships of planktonic foraminifera collected from surface waters.

810 *Palaeogeography Palaeoclimatology Palaeoecology* 202, 143-152. DOI:
811 10.1016/S0031-0182(03)00633-3.

812 Nürnberg D, Bijma J, and Hemleben C, 1996. Assessing the reliability of magnesium in
813 foraminiferal calcite as a proxy for water mass temperatures. *Geochimica Et*
814 *Cosmochimica Acta* 60, 803-814. DOI: 10.1016/0016-7037(95)00446-7.

815 Nürnberg D and Groeneweld J, 2006. Pleistocene variability of the Subtropical Convergence at
816 East Tasman Plateau: Evidence from planktonic foraminifera Mg/Ca (ODP Site
817 1172A). *Geochem. Geophys. Geosyst.*, 7, Q04P11, DOI:10.1029/2005GC000984.

818 Pahnke K, Zahn R, Elderfield H, Schulz M, 2003. 340,000-Year Centennial-Scale Marine
819 Record of Southern Hemisphere Climatic Oscillation. *Science* 15. Vol. 301, Issue
820 5635, pp. 948-952. DOI: 10.1126/science.1084451.

821 Paul A, Mulitza S, Pätzold J and Wolff T, 1999. Simulation of oxygen isotopes in a global
822 ocean model, from *Fisher G, Wefer G. (eds), Use of Proxies in paleoceanography:*
823 *Examples from the South Atlantic.* Springer-Verlag Berlin Heidelberg, pp 655-686.
824 DOI :10.1007/978-3-642-58646-0_27.

825 R Development Core Team (2019). R: A language and environment for statistical computing.
826 R Foundation for Statistical Computing, Vienna, Austria. URL [https://www.R-](https://www.R-project.org/)
827 [project.org/](https://www.R-project.org/).

828 Rathburn AE and DeDecker P, 1997. Magnesium and strontium compositions of Recent
829 benthic foraminifera from the Coral Sea, Australia and Prydz Bay, Antarctica. *Marine*
830 *Micropaleontology* 32, 231-248. DOI : 10.1016/S0377-8398(97)00028-5

831 Regenber M, Nürnberg D, Steph S, Groeneveld J, Garbe-Schonberg D, Tiedemann R, Dullo
832 WC, 2006. Assessing the effect of dissolution on planktonic foraminiferal Mg/Ca ratios:
833 Evidence from Caribbean core tops. *Geochemistry Geophysics Geosystems* 7. DOI :
834 10.1029/2005GC001019.

835 Regenber M, Steph S, Nürnberg D, Tiedemann R, Garbe-Schonberg D, 2009. Calibrating
836 Mg/Ca ratios of multiple planktonic foraminiferal species with delta O¹⁸-calcification
837 temperatures: Paleothermometry for the upper water column. *Earth and Planetary*
838 *Science Letters* 278: 324-336. DOI : 10.1016/j.epsl.2008.12.019.

839 Reichart GJ, Jorissen F, Anschutz P and Mason PRD, 2003. Single foraminiferal test chemistry
840 records the marine environment. *Geology* 31, 355-358. DOI:10.1130/0091-
841 7613(2003)031<0355:SFTCRT>2.0.CO;2.

842 Reynolds RW, NA Rayner, TM Smith, DC Stokes, and W Wang, 2002. An Improved In Situ
843 and Satellite SST Analysis for Climate. *J. Climate*, 15, 1609-1625. DOI:10.1175/1520-
844 0442(2002)

845 Rohling EJ, 2000. Paleosalinity: confidence limits and future applications. *Marine Geology*
846 163, 1-11. DOI: 10.1016/S0025-3227(99)00097-3.

847 Rosenthal Y, Boyle EA and Labeyrie L, 1997. Last glacial maximum paleochemistry and
848 deepwater circulation in the Southern Ocean: Evidence from foraminiferal cadmium.
849 *Paleoceanography* 12, 787-796. DOI: 10.1029/97PA02508.

850 Sadekov A, Eggins SM, De Deckker P, Kroon D, 2008. Uncertainties in seawater thermometry
851 deriving from intratest and intertest Mg/Ca variability in *Globigerinoides ruber*.
852 *Paleoceanography* 23. DOI: 10.1029/2007PA001452.

853 Schmidt GA, 1999. Error analysis of paleosalinity calculations. *Paleoceanography* 14, 422-
854 429. DOI: 10.1029/1999PA900008.

855 Schmidt MW, Spero HJ and Lea DW, 2004. Links between salinity variation in the Caribbean
856 and North Atlantic thermohaline circulation. *Nature* 428, 160-163. DOI:
857 10.1038/nature02346.

858 Shackleton NJ, 1967. Oxygen isotope analyses and Pleistocene temperatures re-assessed,
859 *Nature* 215, 15–17. DOI: 10.1038/21015a0.

860 Shackleton NJ, 1968. Depth of Pelagic Foraminifera and Isotopic Changes in Pleistocene
861 Oceans. *Nature*, 218, 79-80. DOI : 10.1038/218079a0.

862 Shackleton, NJ, 1974. Attainment of isotopic equilibrium between ocean water and the
863 benthonic foraminifera genus *Uvigerina*: isotopic changes in the ocean during the last
864 glacial. *Colloques Internationaux du Centre National du Recherche Scientifique*, 219,
865 203-210. hdl:10013/epic.41396.d001.

866 Spero, H. J., & DeNiro, M. J. (1987). The influence of symbiont photosynthesis on the $\delta^{18}\text{O}$
867 and $\delta^{13}\text{C}$ values of planktonic foraminiferal shell calcite. *Symbiosis*, 4, 213-228.

868 Spero HJ, Mielke KM, Kalve EM, Lea DW and Pak DK, 2003. Multispecies approach to
869 reconstructing eastern equatorial Pacific thermocline hydrography during the past 360
870 kyr. *Paleoceanography* 18. DOI:10.1029/2002PA000814, 2003.

871 Spezzaferri S, Kucera M, Pearson PN, Wade BS, Rappo S, Poole CR, Morard R, Stalder C.
872 2015. *PloS ONE*. 2015; 10 (5): e0128108. DOI: 10.1371/journal.pone.0128108.

873 Thirumalai K, Quinn TM, Marino G 2016. Constraining past seawater $\delta^{18}\text{O}$ and temperature
874 records developed from foraminiferal geochemistry. *Paleoceanography* (2016). DOI:
875 10.1002/2016PA002970

876 Tierney JE, Haywood AM, Feng R, Bhattacharya T, Otto-Bliesner BL (2019): Pliocene SSTs
877 and alkenone saturation indices. *Geophysical Research Letters*, 46, 9136–9144.
878 DOI:10.1594/PANGAEA.904916.

879 Toyofuku T, Kitazato H, Kawahata H, Tsuchiya M, and Nohara M, 2000. Evaluation of Mg/Ca
880 thermometry in foraminifera: Comparison of experimental results and measurements in
881 nature. *Paleoceanography* 15, 456-464. DOI :10.1029/1999PA000460.

882 Vinogradova N, Lee T, Boutin J, Drushka K, Fournier S, Sabia R, Stammer D, Bayler E , Reul
883 N, Gordon A, Melnichenko O, Li LF, Hackert, E, Martin M, Kolodziejczyk N, Hasson
884 A, Brown S ; Misra S; Lindstrom E, 2019. Satellite Salinity Observing System: Recent
885 Discoveries and the Way Forward NASA. *Frontiers in Marine Science*. *Front. Mar. Sci.*
886 6: 243. DOI: 10.3389/fmars.2019.00243.

887 Weldeab S, Schneider RR, Kölling M and Wefer G, 2005. Holocene African droughts relate to
888 eastern equatorial Atlantic cooling. *Geology* 33, 981-984. DOI: 10.1130/G21874.1.

889 Weldeab S, Lea DW, Schneider RR, and Anderson N, 2007. 155,00 years of west African
890 monsoon and ocean thermal evolution. *Science* 316, 130301307.
891 DOI:10.1126/science.1140461.

892 Wyceh JB, Clay Kelly D, Kitajima K, Kozdon R, Orland IJ, Valley JW. 2018. Combined effects
893 of gametogenic calcification and dissolution on $\delta^{18}\text{O}$ measurements of the planktic
894 foraminifer *Trilobatus sacculifer*. *Geochemistry Geophysics Geosystems* 19, 4487-
895 4501. DOI :10.1029/2018GC007908.

896
897
898
899
900
901
902
903
904
905
906

907
 908
 909
 910
 911
 912
 913
 914

Table 1. Measured temperature, salinity, DIC, ALK, and $\delta^{18}\text{O}_w$ of the stations selected for this study (October/November 2005).

Stations	Latitude	Longitude	Measured T°C (±0.05) Oct/Nov.	Salinity (±0.05)	DIC (μmol/kg) precision 1μm/Kg accuracy 2 μm/Kg	Alkalinity (μmol/kg) precision 1.5 μm/Kg accuracy 4 μm/Kg	$\delta^{18}\text{O}_w$ (PDB) precision 0.1 ‰ accuracy 0.2 ‰
25	22°38.640'N	20°23.578'W	24.91	36.63	2069	2391	1.1
29	18°8.088'N	20°55.851'W	26.09	36.24	2037	2369	0.9
31	14°32.128'N	20°57.251'W	28.24	35.78	2009	2330	0.8
35	10°23.424'N	20°4.869'W	29.73	35.63	1982	2304	1.2
38	7°2.114'N	17°27.818'W	29.43	34.67	1929	2257	0.7
40	4°22.323'N	15°16.911'W	28.47	34.35	1915	2214	0.8
42	2°15.702'N	13°33.854'W	27.56	35.72	2002	2332	1.1
46	1°35.741'S	10°33.846'W	25.91	36.13	2053	2346	1.0
49	4°44.752'S	8°6.641'W	24.59	36.07	2057	2369	0.9
52	8°6.086'S	5°29.077'W	23.80	35.99	2062	2360	0.7
56	11°51.783'S	2°30.743'W	22.18	36.38	2071	2387	1.0
62	17°59.620'S	2°25.321'E	19.11	35.99	2100	2369	1.1
66	22°26.998'S	6°6.922'E	18.71	35.68	2070	2349	1.0

915
 916
 917
 918
 919
 920
 921
 922
 923
 924
 925
 926
 927

928
 929
 930
 931
 932 **Table 2.** Mean elemental (Mg/Ca and Sr/Ca) and isotopic ($\delta^{18}\text{O}_c$) composition per station, measured
 933 in foraminiferal calcite in mmol/mol and ‰ PDB, respectively. Elemental and isotopic compositions
 934 were determined on the same material (n varying from 5 to 13 specimens per station); isotopic analyses
 935 were done in duplicate for each station. Mean $\delta^{18}\text{O}_c$ - $\delta^{18}\text{O}_w$ measured per stations in ‰ PDB.
 936

Stations	Measured Mg/Ca mmol/mol	Measured Sr/Ca mmol/mol	Measured $\delta^{18}\text{O}_c$ ‰ (V-PDB) precision 0.08‰	Measured $\delta^{18}\text{O}_c$ - $\delta^{18}\text{O}_w$ ‰ (V-PDB)	Recons. $\delta^{18}\text{O}_w$ (Mulitza) ‰ (V-PDB)	Recons. $\delta^{18}\text{O}_w$ (Spero) ‰ (V-PDB)	Recons. $\delta^{18}\text{O}_w$ (this study) ‰ (V-PDB)
25	3.22 ± 0.51	1.53 ± 0.08	-1.76	-2.82	0.38	0.40	0.88
29	4.01 ± 0.24	1.52 ± 0.06	-1.75	-2.63	1.00	0.87	1.44
31	4.78 ± 0.37	1.56 ± 0.18	-2.51	-3.33	0.73	0.49	1.11
35	5.46 ± 0.38	1.59 ± 0.08	-2.35	-3.59	1.27	0.94	1.62
38	4.31 ± 1.14	1.58 ± 0.14	-2.89	-3.59	0.07	-0.10	0.49
40	4.07 ± 0.64	1.57 ± 0.07	-2.98	-3.78	-0.18	-0.32	0.25
42	3.79 ± 0.49	1.53 ± 0.08	-2.38	-3.44	0.21	0.12	0.67
46	3.92 ± 1.24	1.47 ± 0.07	-1.67	-2.66	1.02	0.91	1.46
49	2.99 ± 0.39	1.55 ± 0.11	-1.83	-2.74	0.10	0.16	0.62
52	2.97 ± 0.30	1.50 ± 0.03	-1.34	-2.08	0.57	0.64	1.09
56	3.31 ± 0.53	1.50 ± 0.03	-1.06	-2.10	1.15	1.15	1.65
62	2.20 ± 0.24	1.47 ± 0.07	-0.70	-1.76	0.38	0.64	0.99
66	1.66 ± 0.17	1.48 ± 0.09	-0.74	-1.75	-0.46	-0.02	0.23

937
 938
 939
 940
 941
 942
 943
 944
 945

946
947
948

Table 3. Calibration equations for *T. sacculifer*.

Source			R ²	p-values
Mg/Ca Relationship with Temperature				
This study	Mg/Ca=0.42(±0.13)e^{(T*0.083(±0.001))}	Eq. 1	0.86	2.9e-06
Nürnberg et al., 1996	Mg/Ca=0.37(±0.065)e ^{(T*0.091(±0.007))}		0.93	
Anand et al., 2003	Mg/Ca=1.06(±0.021)e ^{(T*0.048(±0.012))}			
Regenberg et al., 2009	Mg/Ca=0.6(±0.16)e ^{(T*0.075(±0.006))}			
Sr/Ca Relationship with Temperature				
This study	Sr/Ca=(0.0094±0.002)*T+(1.29 ± 0.05)	Eq. 2	0.67	5.e-04
Mg/Ca and Sr/Ca Relationship with Temperature				
This study	T=(-27±15)+(8±1)*ln(Mg/Ca)+(28±11)*Sr/Ca	Eq. 3	0.93	2 e-04
Me/Ca Relationship with Temperature and Salinity				
This study (Mg/Ca)	Mg/Ca=exp((-5.10±2)+(0.09±0.009)*T+(0.11±0.05)*S)		0.91	5.e-06
This study (Sr/Ca)	Sr/Ca = (1.81±0.5) + (0.008±0.002) T - (0.01±0.01)*S		0.71	0.002
δ¹⁸O Relationship with Temperature				
This study	T= 12.08(±1.46)-4.73(±0.51)*(δ¹⁸O_c -δ¹⁸O_w)	Eq. 4	0.88	1.6 e-06
Erez and Luz, (1983)	T= 16.06(±0.549)-5.08(±0.32)*(δ ¹⁸ O _c -δ ¹⁸ O _w)			
Mulitza et al., (2003)	T= 15.35(±0.71)-4.22(±0.25)*(δ ¹⁸ O _c -δ ¹⁸ O _w)			
Spero et al., (2003)	T= 12-5.67*(δ ¹⁸ O _c -δ ¹⁸ O _w)			
measured δ¹⁸O vs. measured Salinity (this study)	δ¹⁸O_w = (0.171±0.04)*S - (4.93 ±1.66)	Eq. 5	0.38	1.2 e-03
direct linear fit to reconstruct salinity based on measured variables (Mg/Ca and δ¹⁸O_c)	S = -0.16 (±0.02) e^(- δ¹⁸O_c)+ 0.28 (±0.1) Mg/Ca+35.80 (±0.33)	Eq. 6	0.82	< 2e-04

949
950
951
952
953
954
955
956
957
958
959
960

961

962 **Table 4.** Temperature, salinity and $\delta^{18}\text{O}_w$ of the stations used to determine the salinity/ $\delta^{18}\text{O}_w$

963 relationship (equation 5)

Stations	Latitude	Longitude	T°C(±0.05)	Salinity(±0.05)	$\delta^{18}\text{O}_w$ (SMOW) precision 0.1% accuracy 0.2%
19	33°20.14'N	14°38.45'W	22.09	36.83	1.3
21	30°23.42'N	16°24.99'W	23.01	36.91	1.4
23	25°20.68'N	18°4.17'W	24.87	37.01	1.8
25	22°38.64'N	20°23.58'W	24.91	36.63	1.3
29	18°8.09'N	20°55.85'W	26.09	36.24	1.1
31	14°32.13'N	20°57.25'W	28.24	35.78	1.1
35	10°23.424'N	20°4.869'W	29.73	35.63	1.5
36	9°5.71'N	19°14.21'W	29.29	35.63	1.1
37	7°43.88'N	18°5.42'W	29.25	34.92	1.0
38	7°2.11'N	17°27.82'W	29.43	34.67	1.0
39	5°49.51'N	16°29.68'W	29.34	34.34	1.0
40	4°22.32'N	15°16.91'W	28.47	34.35	1.1
42	2°15.70'N	13°33.85'W	27.56	35.72	1.3
43	0°57.53'N	12°33.06'W	26.48	36.05	1.3
46	1°35.74'S	10°33.85'W	25.91	36.13	1.3
47	2°17.53'S	10°1.35'W	26.16	36.2	1.2
49	4°44.75'S	8°6.64'W	24.59	36.07	1.2
51	6°55.67'S	6°24.31'W	24.28	36.01	1.1
52	8°6.09'S	5°29.08'W	23.8	35.99	1.0
56	11°51.79'S	2°30.74'W	22.18	36.38	1.3
62	17°59.62'S	2°25.32'E	19.11	35.99	1.3
66	22°26.99'S	6°6.92'E	18.71	35.68	1.3
69	25°0.20'S	8°17.16'E	18.19	35.64	0.9
72	27°2.39'S	10°35.53'E	18.5	35.64	1.0

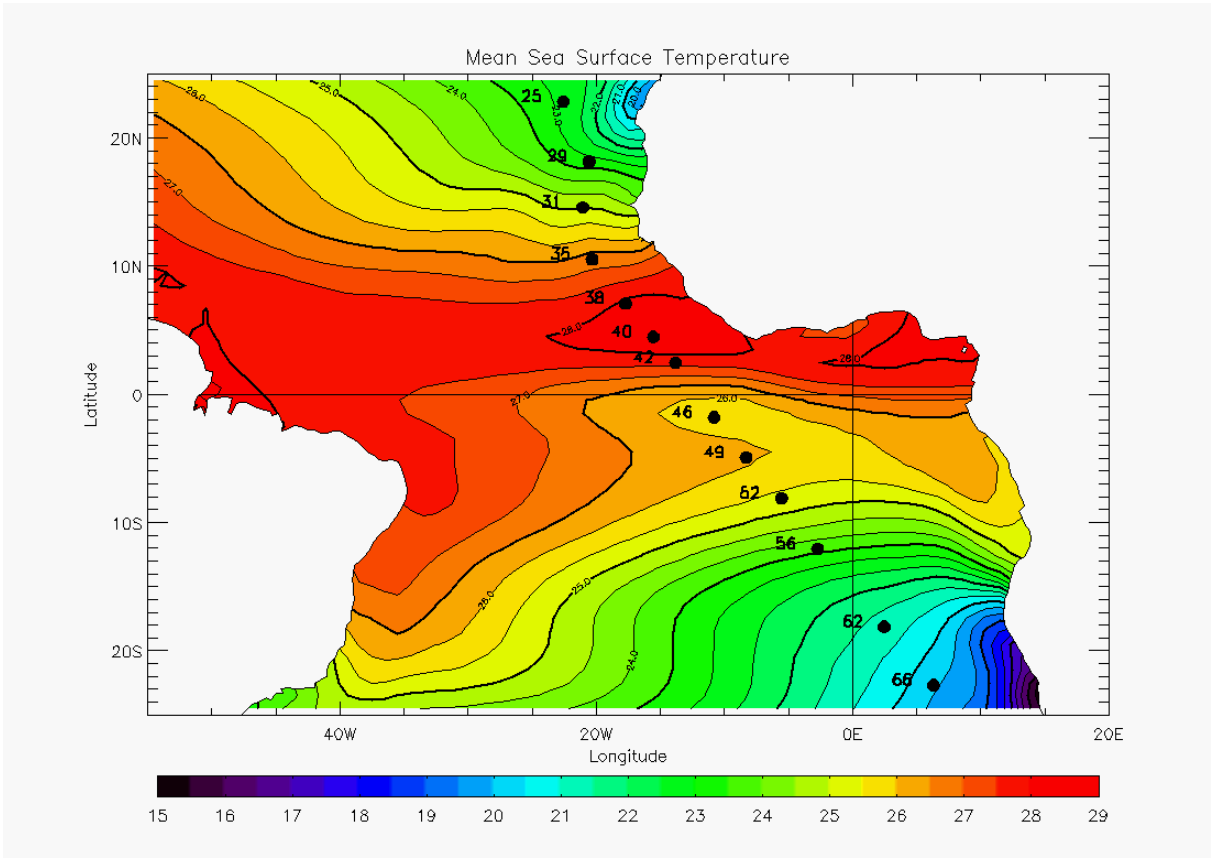
964

965

966

967

968



969
 970
 971
 972

Figure 1a

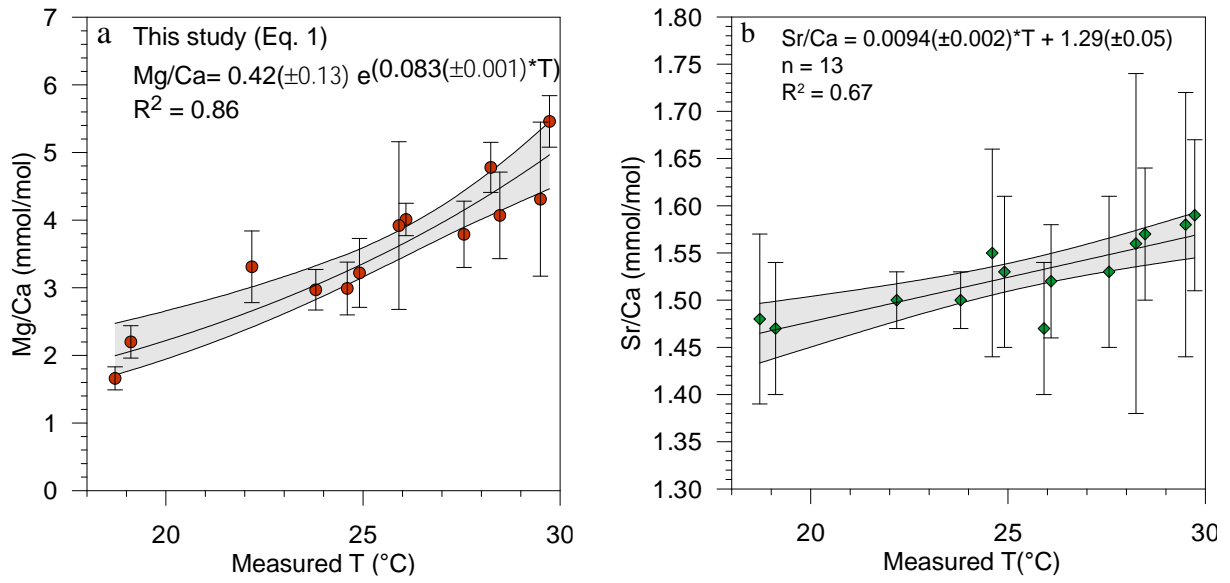


973
 974
 975
 976
 977

Figure 1b

978

979



980

981

982

983

984

985

986

987

988

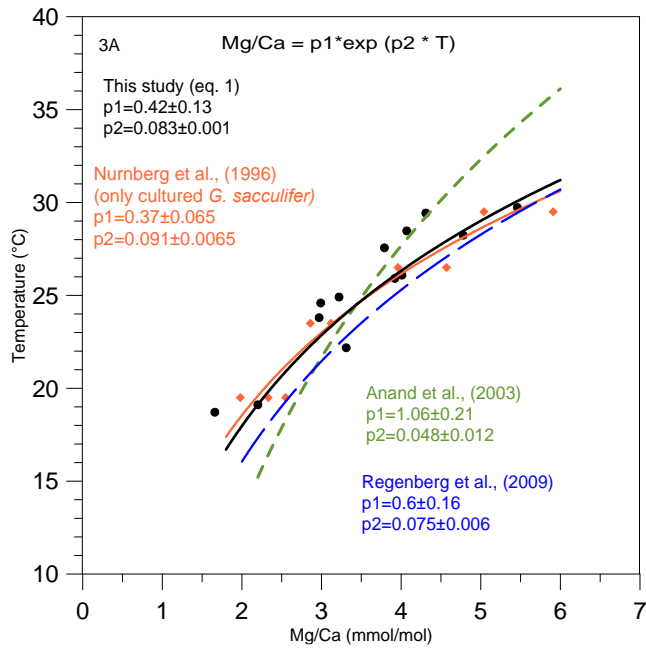
989

990

991

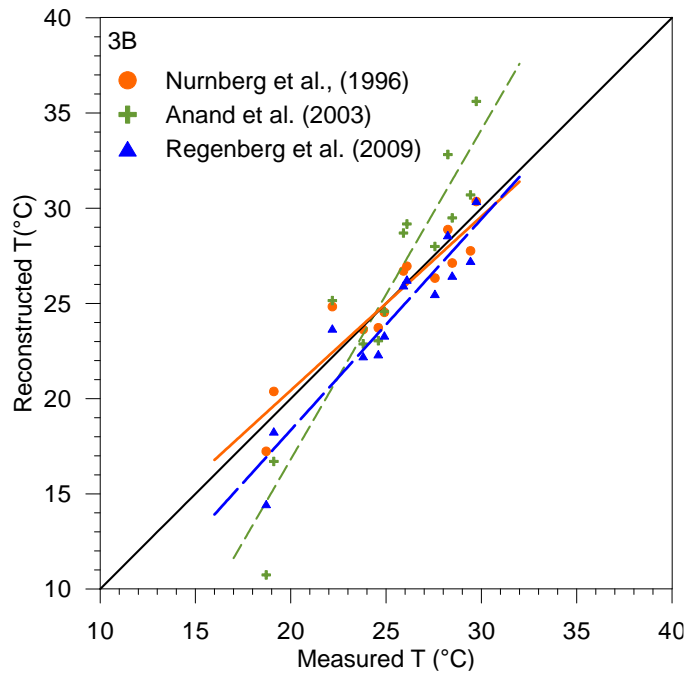
992

Figure 2



993

994



995

996

997

998

999

1000

1001

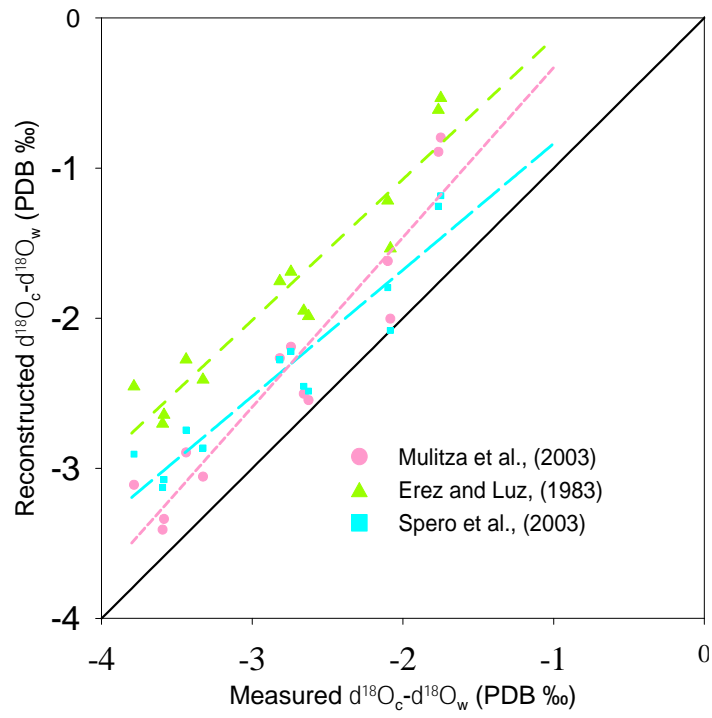
1002

1003

Figure 3

1004

1005



1006

1007

1008

1009

1010

1011

1012

1013

1014

1015

1016

1017

1018

Figure 4

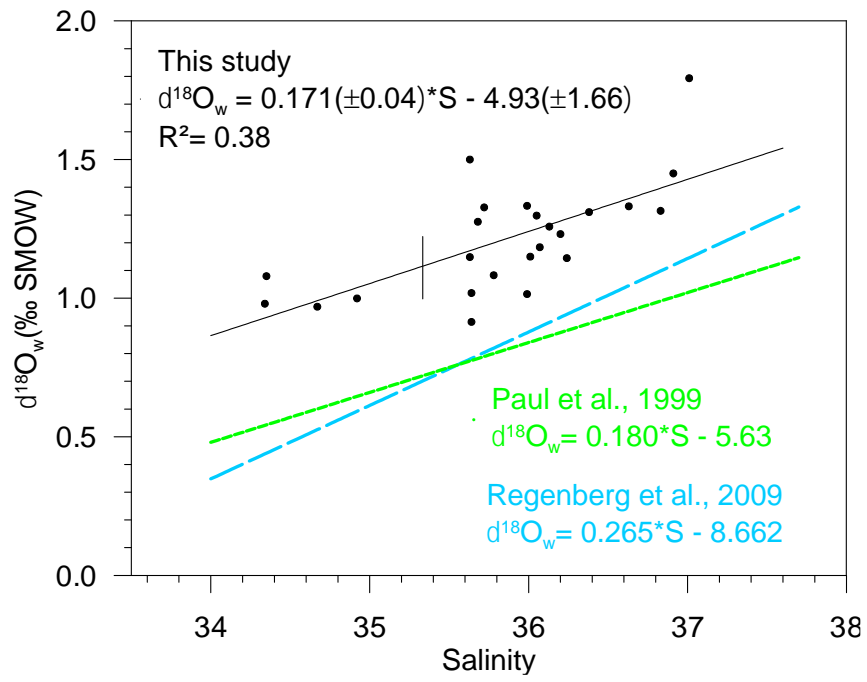
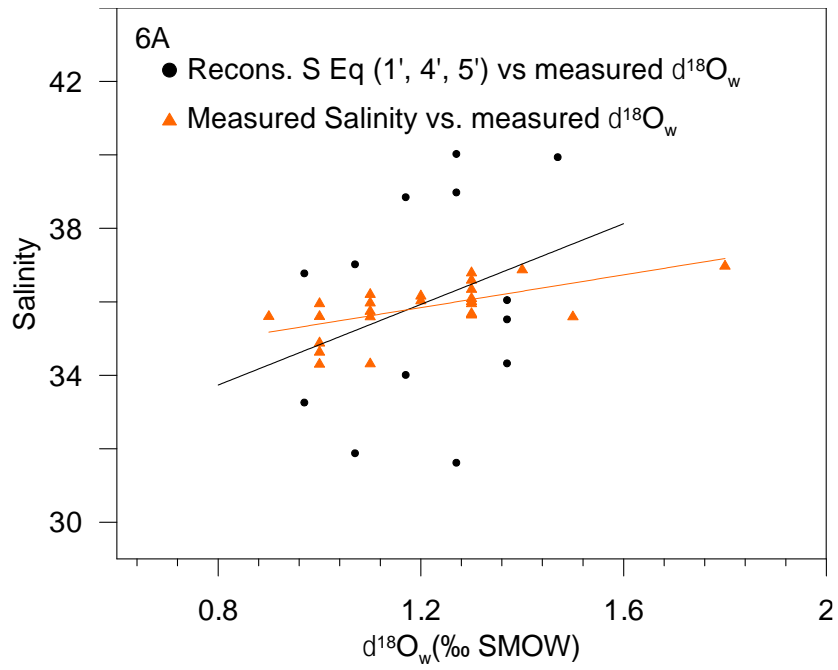


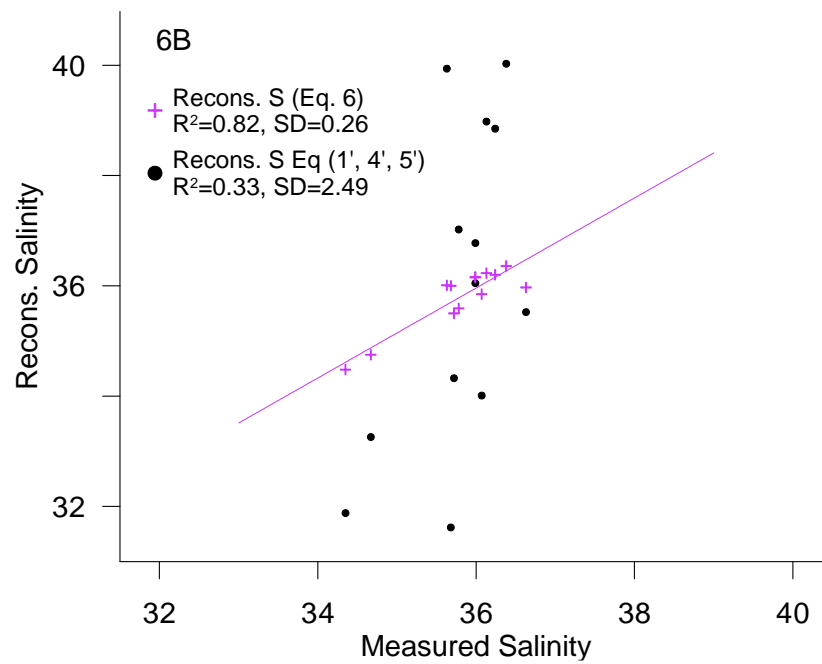
Figure 5

1019
 1020
 1021
 1022
 1023
 1024
 1025
 1026
 1027
 1028
 1029
 1030
 1031
 1032
 1033
 1034
 1035
 1036
 1037
 1038



1039

1040



1041

1042

1043

1044

1045

1046

1047

1048

1049

Figure 6

FIGURE LEGENDS

1050
1051
1052
1053
1054
1055
1056
1057
1058
1059
1060
1061
1062
1063
1064
1065
1066
1067
1068
1069
1070
1071
1072
1073
1074
1075
1076
1077
1078
1079
1080
1081

Fig. 1: Stations used in this study, plotted on gridded data set Reynolds et al., (2002) (a). Set up for planktonic foraminifera collections (b).

Fig. 2: (a) Mg/Ca and (b) Sr/Ca (mmol/mol) and 95% confidence intervals plotted versus measured surface temperature (°C). Each point represents an average of the Mg/Ca and Sr/Ca per station.

Fig. 3 a) Mg/Paleo-temperature equations established in this study (equation 1) (black dots, and full lines), based on the data of Nürnberg et al., (1996) (Orange diamond and large full orange line); Anand et al., (2003) (small green dotted line) and Regenberg et al., (2009) (large blue dotted line) and **3b)** Reconstructed Mg-temperatures (Oct/Nov. 2005) plotted versus measured temperatures (°C) presented in Table 1. For each station mean measured Mg/Ca was inserted into the equation of Nürnberg et al., (1996) (only cultured specimens of *T. sacculifer*) (orange dots, full line), the equation of Anand et al., (2003) (green crosses, small dashed line), and the equation of Regenberg et al., (2009) (blue triangles, large dashed lines).

Fig. 4: Reconstruction of $\delta^{18}\text{Oc}-\delta^{18}\text{Ow}$ by inserting the measured temperature into three $\delta^{18}\text{O}$ based paleo-T-equation: The equation of Spero et al., (2003) (light blue squares, large light blue dashed line), the equation of Mulitza et al., (2003) (pink dots, small pink dashed line), the equation sorted by Erez and Luz (1983) (green triangles, green dashed line) plotted versus measured $\delta^{18}\text{Oc}-\delta^{18}\text{Ow}$ (‰ PDB). The diagonal line represents the 1:1 regression.

Fig. 5: Measured surface $\delta^{18}\text{Ow}$ (‰ SMOW) plotted versus measured surface salinity (stations listed in Tab. 4) (black dots and full line). Regression lines of the $\delta^{18}\text{Ow}$ -salinity relationship calculated by Paul et al., (1999) for the tropical Atlantic Ocean (from 25°S to 25°N) based on GEOSECS data (green line), and by Regenberg et al., (2009) (blue dashed line) based on Schmidt (1999) data for the Atlantic Ocean for the water depth interval of 0–100 m.

Fig. 6: a) Measured salinity (orange triangles) and reconstructed salinity based on equations 1, 4 and 5 from the present study (black dots), plotted versus measured $\delta^{18}\text{Ow}$.

1082 b) Reconstructed salinity based on 1) successive reconstructions using equations 1, 4 and 5
1083 from the present study (black dots) and 2) direct linear fit (Eq. 6) based on the same measured
1084 variables (Mg/Ca and $\delta^{18}Oc$) (purple crosses), plotted versus measured salinity.

1085

1086

1087

1088

1089

1090